TECHNICAL REPORT 7101-3

DRAG REDUCTION AND DIFFUSION ACCOMPANYING THIN SLIT INJECTIONS OF A DRAG REDUCING POLYMER ON A FLAT PLATE AT HIGH REYNOLDS NUMBERS

By

Daniel H. Fruman and
Marshall P. Tulin

June 1972

HYDRONAUTICS, incorporated
research in hydrodynamics

Research, consulting, and advanced engineering in the fields of NAVAL and INDUSTRIAL HYDRODYNAMICS. Offices and Laboratory in the Washington, D. C. area: Pindell School Road, Howard County, Laurel, Md.

571

HYDRONAUTICS, Incorporated

TECHNICAL REPORT 7101-3

DRAG REDUCTION AND DIFFUSION ACCOMPANYING THIN SLIT INJECTIONS OF A DRAG REDUCING POLYMER ON A FLAT PLATE AT HIGH REYNOLDS NUMBERS

By

Daniel H. Fruman and
Marshall P. Tulin

June 1972

Prepared for

Office of Naval Research
Department of the Navy
Under
Contract No. N00014-71-C-0063
NR 062-325

UNCLASSIFIED
Security Classification

DOCUMENT CONTROL DATA - R & D

(Security classification of title, body of abstract and indexing annotation must be entered when the overall report is classified)

1 ORIGINATING ACTIVITY (Corporate author)
HYDRONAUTICS, Incorporated
7210 Pindell School Road, Howard County,
Laurel, Maryland 20810

2a. REPORT SECURITY CLASSIFICATION
Unclassified

2b. GROUP

3 REPORT TITLE
DRAG REDUCTION AND DIFFUSION ACCOMPANYING THIN SLIT INJECTIONS OF A DRAG REDUCING POLYMER ON A FLAT PLATE AT HIGH REYNOLDS NUMBERS

4 DESCRIPTIVE NOTES (Type of report and inclusive dates)
Technical Report

5 AUTHOR(S) (First name, middle initial, last name)
Daniel H. Fruman and Marshall P. Tulin

6. REPORT DATE	7a. TOTAL NO. OF PAGES	7b. NO. OF REFS
June 1972	58	21

8a. CONTRACT OR GRANT NO.	9a ORIGINATOR'S REPORT NUMBER(S)
N00014-71-C-0063 NR 062-325	T. R. 7101-3
b. PROJECT NO.	
c.	9b. OTHER REPORT NO(S) (Any other numbers that may be assigned this report)
d.	

10. DISTRIBUTION STATEMENT
This document has been approved for public release and sale; its distribution is unlimited.

11 SUPPLEMENTARY NOTES	12. SPONSORING MILITARY ACTIVITY
	Office of Naval Research Department of the Navy

13 ABSTRACT

The drag reduction and diffusion accompanying a thin tangential jet injection of an aqueous solution of drag reducing polymer, Polyox WSR 301, into the water turbulent boundary layer of a flat plate at a high free stream Reynolds number, 3.6×10^7, is investigated for a variety of injected concentrations and ratios of injection to free stream velocities. The wall concentration distribution is found to be mainly represented by two regions; the first region where the wall concentration is practically constant and equal to the injected one and the second region where the concentration varies approximately as the inverse of the distance from the injection slit. The length of the first region is highly influenced by the additive and increases linearly with the value of the ejected concentration. It is shown that this increased length is directly related to the thickening of the viscous sublayer observed in homogeneous polymer additive solutions and the changes on the molecular diffusion coefficient attached to high molecular weight polymer at large concentrations. The wall concentration distribution is related to the drag reduction and a simple correlation between its values and the characteristics parameters of the external flow and the drag reducing injection can be established.

ik

DD FORM 1 NOV 68 1473 (PAGE 1)
S/N 0101-807-6801

UNCLASSIFIED
Security Classification

14. KEY WORDS	LINK A		LINK B		LINK C	
	ROLE	WT	ROLE	WT	ROLE	WT
Drag Reduction						
Diffusion Process						
Boundary Layer Ejection						
Polymer Additive						

1c

TABLE OF CONTENTS

LIST OF FIGURES

NOMENCLATURE

Capital Letters

C_f	Local friction factor, $\tau_w/\frac{1}{2}\rho V^2$
D_m	Molecular diffusion coefficient
D_e	Effective diffusion coefficient in turbulent flow
D	Flat Plate drag
DR	Drag reduction (%)
L	Flat Plate length
N	Exponent of the pipe friction law
N_{s_c}	Schmidt number, ν/D_m
R	Pipe radius
Re	Reynolds number
Re_L	Reynolds number for flat plate length
Re_x	Local Reynolds number at x
S_L	Total surface of the flat plate
S_I	Surface of the flat plate from the leading edge to the injection slot
U	Axial velocity in a pipe
V	Free stream velocity in an external flow or mean velocity in a pipe

Lower Case Letters

c	Concentration at the wall
c_i	Injected concentration
ℓ	Length of the initial diffusion zone
n	Exponent of the power law velocity profile
q_s	Sampling discharge
q_D	Discharge through the diffusion sublayer
q_v	Discharge through the viscous sublayer
s	Width of the injection slot
t	Time
u	x-component of the velocity
v	y-component of the velocity
u^*	Shear velocity, $\sqrt{\tau_w/\rho}$
v_i	Injection velocity
x	Distance to the slot measured in the direction of the flow
y	Distance to the wall

Greek Letters

δ	Boundary layer thickness
δ_v	Viscous sublayer thickness

δ_D Diffusion sublayer thickness

$\delta_v^+ = \delta_v u^*/\nu$ - Dimensionless viscous sublayer thickness

$\delta_D^+ = \delta_D u^*/\nu$ - Dimensionless diffusion sublayer thickness

μ Dynamics viscosity

ν Kinematic viscosity

ρ Specific gravity

τ_w Wall shear stress

ψ Stream function

ABSTRACT

The main purpose of this work is to study the diffusion of a thin tangential jet of an aqueous solution of drag reducing polymer injected into the water turbulent boundary layer of a flat plate at a free stream Reynolds number, 3.6×10^7, and at the same time to measure the accompanying drag reduction. Measurements of the concentration of injected fluid at the wall of the flat plate, at different stations downstream from the narrow injection slit, were performed for a variety of initial concentrations and ratios of injection to free stream velocities. The injection slit is located downstream of the leading edge in a region where the boundary layer is already turbulent. Due to the fact that direct measurements of the polymer concentration cannot easily be made, the injected solutions were darkened with drawing ink and the concentration of ink was measured by light absorption techniques, using specially designed photocells. In this study, it is supposed that the diffusion of the dye is also representative of the diffusion of the polymer solution. The dye concentration measurements in the case of water injection are close to those found in other studies for the temperature distribution over an insulated flat plate in the case of tangential heated fluid injection into a turbulent boundary layer. For the drag reducing polymer injection, an empirical formula has been obtained where the ratio of measured concentration at a downstream station to the injected concentration is a function of some dimensionless distance.

The wall concentration distribution is found to be mainly represented by two regions; the first region where the wall concentration is practically constant and equal to the injected one and the second region where the concentration varies approximately as the inverse of the distance from the injection slit. The length of the first region is highly influenced by the additive and increases linearly with the value of the ejected concentration. From a simple theoretical analysis, it is shown that this increased length is directly related to the thickening of the viscous sublayer observed in homogeneous polymer additive solutions and the changes on the molecular diffusion coefficient attached to high molecular weight polymer at large concentrations.

It is also shown that the wall concentration distribution is related to the drag reduction and that a simple correlation between its values and the characteristics parameters of the external flow and the drag reducing injection can be established. By applying this correlation to the results published by different authors it is shown that a quite accurate estimation of the injection requirements can be made in a large range of Reynolds numbers.

I. STATEMENT OF THE PROBLEM

The ability of high polymer solutions to reduce the turbulent friction resistance in pipes is well known since the pioneering studies of Toms (1). During the last ten years a broad experimental and theoretical research effort has been made in order to clarify understanding of the phenomena and to study the possible application to naval engineering problems. We refer to the papers of Tulin (2), Lumley (3), Paterson et al. (4) and Hoyt (5) for a complete bibliography on the subject.

Although considerable progress has been made in understanding the subject, actual applications to large ships have not been made, nor have they been proposed too seriously. This was partly due to the fact that theoretical understanding of the dispersion of polymer solutions in turbulent boundary layers at very high Reynolds number was not supported by experimental evidence.

Experimental results are available in the case of wall injection in circular pipes; Wells (6) performed the injection on a completely developed boundary layer, while Poreh (7) injected the polymer solutions in a developing boundary layer. Here we concentrate our attention on drag reduction in flow over flat plates. Love (8) performed experiments in a small recirculating channel, where injection of an aqueous solution of polyethylene oxide Polyox WSR 301 is made on a 0.46 m long flat plate through a 14 degree inclined slit, having a clearance of 0.8 mm and situated at 3.76 cm from the leading edge. The free stream velocities

used were 2.90 and 3.50 m/sec which correspond to Reynolds numbers of 1.28 to 1.7 x 10^6. He showed that a maximum drag reduction of 45 to 50% of the difference between the turbulent and laminar drag can be obtained in this range of Reynolds numbers. The optimum concentration was about 50 ppm and the optimum flow rate about 1.0 x 10^{-3} m^3/sec/m. Wu (9) made a complementary analysis of Love's results and showed that the optimum ejection rate corresponds roughly to the discharge within the inner boundary layer. Later Wu and Tulin (10) gave new experimental evidence of the polymer requirements using a 7 degree inclined slot with gaps varying from 0.56 to 2.36 mm at a free stream velocity of 2.44 m/sec and a flat plate Reynolds number of 1.3 x 10^6. Their results indicate that for the smallest gap a higher drag reduction than found by Love for the same Reynolds number (1.3 x 10^6) can be obtained by using an ejection of 500 ppm solution of the same polymer at a flow rate of only 0.1 x 10^{-3} m^3/sec/m. In fact the polymer consumption is practically the same in the two tests; a decrease on the injection rate requires an increase on the concentration and vice-versa. We must point out that the ratio between the ejection and the free stream velocity is in the case of Love of 0.42 and only 0.098 for the reported tests of Wu and Tulin.

In the same range of Reynolds numbers (0.8 to 2.2 x 10^6), Tagori and Ashidate (11) performed injection tests on a 2.505 m flat plate in a free surface channel using the same polymer as drag reducing additive. The injections were performed tangentially through a 1.5 mm width slit at flow rates varying from

0.01 10-3 to 0.13 x 10^{-3} m^3/sec/m and concentrations from 50 to 500 ppm. Their results are summarized in a formula having a range of application limited to the values of parameters mentioned above. For Reynolds numbers exceeding their upper value, e.g. 10^7, the drag reduction computed by using this suggested formula are unreasonably high.

Because the drag reduction which can be obtained from a given high polymer injection is related closely to the diffusion of the drag reducing agent into the turbulent boundary layer and consequently to the concentration distribution along the wall, it seemed of interest to perform experiments and measure simultaneously this distribution and the associated drag reduction. High free-stream Reynolds numbers were choosen to perform these experiments in order to be in a range of parameters close to those of some possible practical applications: torpedo, hydrofoil, screw propeller, etc.

This report is divided in several sections as follows: Section II is a description of the experimental set-up and the methods of analysis of the drag reduction and concentration measurement data. Section III is devoted to the presentation of the experimental data along with a tentative correlation of the concentration measurements data. Section IV presents a discussion of the physics of the diffusion process according to our experimental evidence and together with the well known viscous sublayer thickening and boundary layer velocity distribution effects due to polymer additives. Finally Section V is

devoted to the correlation of the available drag reduction data with the trailing edge concentration computed by using the results of Section III.

II. EXPERIMENTAL SET-UP

The flat plate used was 3.048 m long and 5.08 cm thick with a well rounded leading edge and a sharp trailing edge as shown in Figure 1. The injection slot was located at 0.23 m from the leading edge and was 0.30 m in height and 0.5 mm wide. As is shown in Figure 1, the slot was designed with a view to ensure a tangential flow with the minimum disturbance of the upstream velocity profile. Five sampling slits were located at middepth of the plate at 0.063, 0.203, 0.508, 1.007 and 2.337 m from the injection slot. The dimensions of those sampling slits were 0.038 m long and 0.25 mm wide.

The tests were performed in the HYDRONAUTICS High Speed Channel (HSC) at a constant free stream velocity of 10.65 m/sec. The plate was mounted in a Planar Motion Mechanism (PMM) (12) system and reluctance force gages were used to measure the drag. The output of the gages was integrated during a certain period of time (2 seconds) before and during each injection in order to obtain the mean values of the drag forces.

The injection system consists of an injection reservoir having a total volume of 0.137 m^3 connected with three independent distributors inside the plate through a stopcock and a

manifold. The flow rate was computed by measuring the change on the reservoir level during a known time interval.

The sampling system consists of a vacuum pump, a vacuum reservoir, three photocells (13) and a sampling reservoir (Figure 2). The concentrations were recorded continuously by means of a U.V Visicorder. Because only three cells were used for five sampling slits it was necessary to provide two of these with a by-pass. When the shift from one slit to another slit was made the fluid sampled from the first slit and contained in a small portion of the tubing diffusesinto the sampling stream arriving from the second slit and could change the value of the measured actual concentration. This is especially true when the first slit is choosen to be upstream of the second slit. During the tests made with the three lower concentrations the order of sampling was such that the first three slits were sampled at the beginning and the last slits at the end of the run. This order was changed during the subsequent tests in order to reduce the influence of the higher dye concentrations of the upstream on the downstream slits. For these tests, samples from the first, fourth and fifth slits were measured at the beginning and from the second and third at the end.

II.1 Drag Measurements

The drag reduction takes place only on the surface effectively covered by the injection and it was therefore necessary to infer the value of the drag of this surface from

the net drag measurement without injection. Such measurements were made for different velocities and the results are shown in Figure 3. These values are distinctly different from those corresponding to a conventional flat plate. This is due to the fact that, although the wave making and pressure drag can be neglected in the present case, there is an important component associated with the splash of the water at the leading edge of the plate, since the plate is only partly submerged in the channel. To take into account this effect the plate was tested at the same velocity, 10.65 m/sec, but at different depths in order to obtain by extrapolation the value of the splash drag for zero depth. Figure 4 is a plot of these different values of the drag versus the depth of immersion. For zero depth the residual drag is about 8.0 Kg. By subtracting this value from those obtained at the depth used in our tests, 0.304 m, we compute a drag coefficient of 0.242×10^{-3}, which is very close to the friction drag coefficient calculated according to conventional formulas(Figure 3).

It can be then inferred that the friction drag of the surface of the flat plate covered by the injection could be accurately computed by using for the laminar drag the following formula,

$$D_{Lam} = 1.328 \times \frac{1}{2}\rho V^2 \left[Re_L^{-1/2} S_L - Re_I^{-1/2} S_I \right], \qquad [1]$$

and for the turbulent drag

$$D_{Turb} = 0.074 \times \frac{1}{2}\rho V^2 \left[Re_L^{-1/5} S_L - Re_I^{-1/5} S_I \right] \qquad [2]$$

where R_L, S_L and R_I, S_I are respectively the Reynolds number and the wetted surface corresponding to the total length of the plate and the injection station. Let ΔD be the difference between the drag measured before and during the injection; the drag reduction effectiveness will be defined by

$$DR(\%) = \frac{\Delta D}{D_{Turb} - D_{Lam}} \times 100 \; . \qquad [3]$$

Two measurements of the velocity were made for each test; one by using a Prandtl tube placed between the plate and one of the walls of the channel and another by means of the pressure drop between two stations in the convergence section of the HSC. The velocity computed from these two independent measurements did not differ by more than two percent. Besides, no appreciable change on the velocity due to the drag reducing injection was observed. The scatter in repeated drag measurements made without injection is less than ±0.5% of the mean value.

II.2 Concentration Measurements

The concentration measurements were made with specially designed light absorption systems and photocells. The input voltage or intensity of the light source was choosen in order to achieve the maximum possible output readings between zero dye and

dye concentration corresponding to practically zero light transmission. This dye concentration was choosen after several tests to be 1250 ppm of India ink in tap water. The corresponding voltage output of the photocell was 40.0 mV and the equivalent spot displacement on the U.V recorder was 12.0 cm. Figure 5 gives the calibration curve for the three cells. It is interesting to see from this figure that the response of the photocell varies non linearly with the concentration. This allows very good precision in the range of low concentrations which are the most interesting in the scope of this work.

The procedure used for continuous sampling can be described as follows. Before each injection the vacuum reservoir was switched on and the Visicorder started in order to obtain an initial reading for the water contained in the channel. These readings were compared with those obtained during the calibration of the cell. After the injection was started the output of the cells were continuously recorded till they reached a steady value. Only at this moment two of the cells are connected to the other slits and continuously recorded till they reached a new steady state. This method of measurement allows a very good precision of the values of the concentration. However some scatter appears in the results; it seems to be due to the errors introduced by different factors as: precision of the dye concentration of the injected solution, coloration of the water used in the channel after several tests, stability of the light intensity, stability

of the galvanometers of the U.V recorder, precision in the readings of the U.V records and calibration curves, etc. In spite of this scatter the general features of the diffusion process may be accurately examined.

II.3 Sampling at the Wall

The fluid sampled by aspiration of the boundary layer close to the flat plate wall will be more or less representative of the wall concentration itself depending on the rate of sampling. For the three cells sampled simultaneously in the experiments the rate of sampling is less than 5.0 cm^3/sec, that is to say 0.43 $cm^3/sec/cm$. The dimensionless boundary layer thickness corresponding to this flow rate will be,

$$y^+ = \left(\frac{2q_s}{\nu}\right)^{\frac{1}{2}} = 9.27$$

value slightly lower than the Newtonian viscous sublayer thickness. For drag reducing fluids the fluid will be sampled from only a small portion of the thickened viscous sublayer which is three times larger than the Newtonian viscous sublayer in the case of maximum drag reduction.

The measurements will then correspond to the bulk concentration inside a thin layer of fluid close to the wall. Because we are in this work mainly interested in the drag reduction effects, which are related to the additive concentration in the viscous sublayer thickness, these concentration measurements can be considered as characteristic of the effect of interest.

II.4 Polymer Used and Mode of Preparation

The polymer used in these tests were polyethylene oxide, Polyox WSR 301, from the Union Carbide Corporation. The solutions to be injected were made by diluting a 1000 ppm master solution, prepared about 24 hours in advance, with the necessary amount of tap water. The dilution was performed just before the tests and the dye (India Ink) was introduced simultaneously. Gentle manual mixing was used to insure a homogeneous solution.

For some of the solutions prepared in such a way it was verified that the light diffusion corresponding to the 1250 ppm of dye was not affected by the dissolved high molecular weight polymers. These readings were very close to those obtained during the photocell calibration using tap water.

III. PRESENTATION OF THE RESULTS

III.1 Drag Reduction Results

Figure 6 shows the values of the drag reduction computed as indicated in Section II.1 as a function of the injection over free stream velocity ratio and additive concentrations. It appears that for constant injection rate the drag reduction increases for 100, 200 and 500 ppm concentration solutions. For tested concentrations larger than the latter - 750 and 1000 ppm - the drag reduction is quite constant and equal to those obtained with 500 ppm. The maximum value of the drag reduction obtained, for the range of injection rates tested, is 56.3%.

It is interesting to compare the present results with those obtained by Wu and Tulin (10) using similar slot width, 0.56 mm, and ratio of injection to free stream velocity. Figure 6 shows that, despite the large difference in the free stream velocities and Reynolds numbers, the values of the drag reduction obtained by these authors are very close to the present results. The consumption of polymer required to obtain the same drag reduction is however very different between these two experiments. In the present case this consumption is about four times larger than in Wu's experiments.

III.2 Concentration Measurements

The results obtained for dyed water injection are shown in Figure 7. Only for the first three sampling slits the concentration measured is high enough to be taken into account. For the last two slits the concentration is less than 1% of the injected concentration. These results can be compared with those obtained by Seban (14) for the wall temperature distribution over an insulated flat plate in the case of a tangential injection of a heated gas into a turbulent boundary layer in air. Seban has shown that for ratios of injection to free stream velocity lower than one the relative temperature distribution can be correlated with a dimensionless distance given by $(\rho V/\rho_i v_i)^{1.5}\ (x/s)$ where ρ and ρ_i are respectively the densities of the free stream and injected fluid.

By using a similar parameter, with $\rho = \rho_i$ in our case, we obtain for the dyed water injection a concentration distribution fit given by,

$$\frac{c}{c_i} = 17.01 \left(\frac{v_i}{V}\right)^{1.06} \left(\frac{x}{s}\right)^{-0.711} \qquad [4]$$

that is to compare with Seban's formula for the temperature distribution

$$\frac{t}{t_i} = 25.0 \left(\frac{\rho_i v_i}{\rho V}\right)^{1.2} \left(\frac{x}{s}\right)^{-0.8} \qquad [5]$$

where t is the wall temperature. Taking into account that our fit is obtained by using only a few experimental points and that the experimental set-ups were quite different, comparison between these two formulae is very satisfactory. This agreement gives confidence in the technique employed for concentration measurements.

The injection of Polyox solution instead of pure water changes completely the measured concentration distribution curves. For low concentrations, say 100 ppm, it can be seen in Figure 8 that a very important downstream shift appears in the decay of concentration. For the same sampling slit and injection velocity the measured concentrations are in this case an order of magnitude larger than in the case of water injection. As might be expected this shift increases with the injection velocity and concentration, Figures 9 to 12.

To be consistent with what was done above for water injection the dimensionless distances, x/s, were multiplied by $(v_i/V)^{-1.5}$ and the mean square fit for all the values of dimensionless concentrations less than 0.8 was computed for each injected concentration. With these fits it is possible to define the effective distances for which $c/c_i = 1$. These points are exhibited in Figure 13 as a function of the injected concentration. Notwithstanding a certain scatter, a linear relationship between the shift of the concentration lines and the injected concentration can be found. If this effective distance is made the basis of the measurements of distance downstream, the concentration distribution for the decay region is given by,

$$\frac{c}{c_i} = 10.79 \left(\frac{v_i}{V}\right)^{1.74} \left(\frac{x}{s}\right)^{-1.16} c_i^{1.16} \qquad [6]$$

Figure 14 shows the experimental points together with the best fit mentioned above. Although the spread of the experimental points are quite substantial for the low concentrations, expression [6] is still a relatively accurate formula that may be found useful in estimating the practical application of drag reducing fluid through thin slit injection.

IV. PHYSICAL DISCUSSION

It seems possible to divide the behavior of the injected wall jet into two regions, i) an upstream region where the diffusion is not very important and ii) a downstream region where the diffusion near the wall is very important and can be approximated by a power law dependence on distance.

i) In the first region, on the assumption that molecular diffusion in the viscous boundary layer is preponderant we can make a simple computation to obtain an approximate value of the length of this region. The path of a fluid particle is given by

$$x = \int u \, dt \qquad [7]$$

The u velocity dependence on the thickness of the viscous sublayer can be written

$$u = \left(\frac{\tau_w}{\mu} \right) y \qquad [8]$$

and y is related to the molecular diffusion, D, by

$$y = (D_m \, t)^{\frac{1}{2}} \qquad [9]$$

By replacing [8] and [9] in [7] and integrating between the wall and the diffusion sublayer, δ_D for τ_w constant on x, we obtain

$$\ell = \frac{2}{3} \frac{\tau_w}{\mu \, D_m} \delta_D^3$$

where ℓ is the length of the initial region. By using dimensionless values of the viscous sublayer thickness we have,

$$\ell = \frac{2}{3} N_{s_c} \delta_D^{+3} \frac{\nu}{u^*} \qquad [10]$$

For a Newtonian fluid and an inert tracer we can estimate the length of this initial region by using the classical relationship between the diffusion and viscous sublayer (15),

$$\delta_D^+ = \frac{\delta_v^{+3/4}}{N_{s_c}^{1/4}} \qquad [11]$$

and by introducing [11] into [10] we obtain

$$\ell = \frac{2}{3} N_{s_c}^{1/4} \delta_v^{+9/4} \frac{\nu}{u^*} \qquad [12]$$

The value of the dimensionless viscous sublayer can be estimated from (16)

$$\delta_v^+ = \frac{u^* \delta_v}{\nu} \simeq 10 \qquad [13]$$

and the wall shear velocity

$$\frac{u^*}{V} = 0.1152 \ Re_x^{-1/10} \qquad [14]$$

Considering that the injection is performed in a region where $Re_x \simeq 2 \times 10^6$, the length of the initial zone will be

$$\ell \simeq 4 \text{ mm} \qquad [15]$$

which correspond to about 8 times the slot width used in our case. This value is close to the experimental results of Seban (14) and our own extrapolated values for low ratios of injection to free stream velocity.

Let us suppose that the Schmidt number is unchanged for the low concentration solutions of high polymers (17). The ratio between the initial zone, due only to the thickening of the viscous sublayer by the additive, will be, denoting by the subscript p the values referring to the polymer solutions,

$$\frac{l_p}{l} = \left(\frac{\delta_{v_p}^+}{\delta_v^+} \right)^{9/4} \frac{u^*}{u^*_p} \qquad [16]$$

By assuming, following experimental evidence (18), that the ratio between the dimensionless viscous sublayer thickness is,

$$\frac{\delta_{v_p}^+}{\delta_v^+} \simeq 3 \qquad [17]$$

and that the ratio between the wall shear velocities (cf.(19) and Appendix) is,

$$\frac{u^*_p}{u^*} \simeq 0.8 \qquad [18]$$

we obtain

$$\frac{l_p}{l} \simeq 15 \qquad [19]$$

It can be expected that diffusivity is very small for such high molecular weight additives at high concentrations and consequently a considerably larger value of the initial zone will be reached. By using the estimation of $D \simeq 10^{-8}$ m²/sec given by Poreh and Hsu (20) Equation [16] becomes if the viscosity is unchanged

$$\frac{\ell_p}{\ell} = \left(\frac{D_m}{D_{m_p}}\right)^{1/4} \left(\frac{\delta_{v_p}}{\delta_v^+}\right)^{9/4} \frac{u^*}{u^*_p} \qquad [20]$$

and its numerical value will be

$$\frac{\ell_p}{\ell} \simeq 85 \quad . \qquad [21]$$

The length of the initial zone will be one or two orders of magnitude larger than for a Newtonian fluid and an inert tracer depending on the assumed values of $(\delta_{v_p}^+/\delta_v^+)$ and (D_m/D_{m_p}). This simple computation shows remarkably good agreement with our experimental results. We can conclude this section by saying that the changes in the viscous sublayer thickness due to the additive together with the decrease on the molecular diffusivity attached to high molecular weight polymers produce a considerable increase on the length of the initial diffusion zone.

ii) In the second or final region turbulent mixing predominates right to the wall. The mass balance can be written

$$u \frac{\partial c}{\partial x} + v \frac{\partial c}{\partial y} = \frac{\partial}{\partial y} \left(D_e \frac{\partial c}{\partial y} \right) \qquad [22]$$

where u and v are the velocities in the direction of x and y respectively, c(x, y) the concentration and D_e the effective diffusion coefficient. This relation can be written in von Mises coordinates (x, ψ) and we obtain

$$\left. \frac{\partial c}{\partial x} \right|_{\psi} = \frac{\partial}{\partial \psi} \left(D_e \, u \frac{\partial c}{\partial \psi} \right) \qquad [23]$$

By assuming that the effective diffusion is given by (15),

$$D_e = \beta \, u^* \, y \qquad [24]$$

and

$$\frac{u}{V} = \left(\frac{y}{\delta} \right)^{\frac{1}{n}} \qquad [25]$$

we have

$$\left. \frac{\partial c}{\partial x} \right|_{\psi} = V^2 \, \delta \frac{\partial}{\partial \psi} \left(\beta \frac{u^*}{V} \left(\frac{y}{\delta} \right)^{1+1/n} \frac{\partial c}{\partial \psi} \right) \qquad [26]$$

and

$$\psi = V \delta \int \frac{u}{V} \, d \left(\frac{y}{\delta} \right) = V \delta \frac{\left(\frac{y}{\delta} \right)^{1+1/n}}{1+1/n} \qquad [27]$$

then, by introducing [27] into [26],

$$\left.\frac{\partial c}{\partial x}\right|_{\psi} = V\beta \frac{n+1}{n} \frac{u^*}{V} \frac{\partial}{\partial \psi} \left(\psi \frac{\partial c}{\partial \psi}\right) \qquad [28]$$

By assuming that the shear velocity, u*, is independent of x, Equation [28] has an exact solution,

$$c = \kappa\, x^{-1}\, e^{-\frac{\psi/Vx}{\beta u^*/V\ (n+1/n)}}$$

$$= \kappa\, x^{-1}\, e^{-\frac{\psi/Vx}{\beta \sqrt{C_f/2}\ (n+1/n)}} \qquad [29]$$

The constant κ is determined by,

$$c_i \frac{v_i\, s}{V\, \delta} = \int_0^{n/n+1} c\, d\psi' \qquad [30]$$

where $\psi' = \psi/V\delta$, is the dimensionless stream function. By operating we obtain,

$$\kappa = -(c_i \delta) \frac{\frac{v_i\, s}{V\, \delta}}{\beta \sqrt{C_f/2}\ (n+1/n) \left[e^{-\frac{(n/n+1)^2}{\beta \sqrt{C_f/2}}} - 1 \right]} \qquad [31]$$

that replaced in [29] allows the computation of the concentration profile through the boundary layer,

$$c = c_i \frac{q_i}{\nu} \frac{1}{Re_x} \frac{1}{\beta\sqrt{\frac{C_f}{2}}\frac{n+1}{n}\left[1 - e^{-\frac{(n/n+1)^2}{\beta\sqrt{C_f/2}}}\right]} e^{-\frac{y'^{\,n+1/n}\,(\delta/x)}{\beta\sqrt{C_f/2}\,(n+1/n)^2}} \qquad [32]$$

where $y' = y/\delta$ is the dimensionless distance from the wall and q_i, the injection rate per unit width. Although it was assumed in the above computation that the wall shear velocity, and consequently the local friction factor, is a weak function of the distance, for purposes of numerical calculation the dependence on local Reynolds number will be taken into account.

For a Newtonian fluid we have (16),

$$\frac{C_f}{2} = 0.0288\ (Re_x)^{-1/5}\ ,$$

$$\frac{x}{\delta} = 2.7\ (Re_x)^{1/5} \qquad [33]$$

for $n = 7$. For a drag reducing fluid and maximum drag reduction efficiency the following formula is derived by simple calculation (see Appendix)

$$c = c_i \frac{q_i}{\nu} \frac{1}{Re_x} \frac{1}{\beta\sqrt{\frac{C_f}{2}}\frac{n+1}{n}\left[1 - e^{-\frac{(n/n+1)^2}{\beta\sqrt{C_f/2}}}\right]} e^{-\frac{y'^{\,n+1/n}}{\beta\sqrt{C_f/2}\,(n+1/n)^2}\frac{(\upsilon/x)}{}} \qquad [32]$$

where $y' = y/\delta$ is the dimensionless distance from the wall and q_i, the injection rate per unit width. Although it was assumed in the above computation that the wall shear velocity, and consequently the local friction factor, is a weak function of the distance, for purposes of numerical calculation the dependence on local Reynolds number will be taken into account.

For a Newtonian fluid we have (16),

$$\frac{C_f}{2} = 0.0288\ (Re_x)^{-1/5}\ ,$$

$$\frac{x}{\delta} = 2.7\ (Re_x)^{1/5} \qquad [33]$$

for n = 7. For a drag reducing fluid and maximum drag reduction efficiency the following formula is derived by simple calculation (see Appendix)

$$\left(\frac{C_f}{2}\right)_p = 0.24\ (Re_x)^{-1/2.75},$$

$$\frac{x}{\delta_p} = 0.415\ (Re_x)^{1/2.75} \qquad [34]$$

for $n_p = 2.5$. By assuming a value of $\beta = 1$ and by replacing [33] or [34] into [32], the concentration distribution through the boundary layer can be easily computed. Figure 15 shows the change in the concentration profile between the pure solvent and the polymer solution for a local Reynolds number 10^7. It is shown that changes between the two profiles appear only in the region far from the wall.

For the concentration distribution along the wall let us consider Fquation [32] for y = 0

$$\frac{c}{c_i} = \frac{v_i}{V}\frac{s}{x}\frac{1}{\beta\sqrt{\frac{C_f}{2}}\left(\frac{n+1}{n}\right)\left[1 - e^{-\frac{(n/n+1)^2}{\beta\sqrt{C_f/2}}}\right]} \qquad [35]$$

By neglecting the exponential term we can analyze the changes in the concentration due to the velocity profile in the case of the inert tracer and the polymer. Let us make the ratio of these concentrations for the same values of injected concentration, velocities and ratio of slot width to distance, for $Re_x = 10^7$

$$\frac{c_p}{c} = \frac{\sqrt{\left(\frac{C_f}{2}\right)\left(\frac{n+1}{n}\right)}}{\sqrt{\left(\frac{C_f}{2}\right)_p\left(\frac{n_p+1}{n_p}\right)}} = \frac{017\ Re_x^{-1/10}\ \frac{8}{7}}{049\ Re_x^{-1/5.5}\ \frac{3.5}{2.5}} \qquad [36]$$

$$\frac{c_p}{c} = 0.284\ Re_x^{0.082} = 0.284\ (10^7)^{0.082} \simeq 1.0$$

We can conclude that, for large enough Reynolds number ($0 \sim 10^7$), the concentration distributions close to the wall for an inert tracer and a drag reducing agent injected tangentially on a turbulent boundary layer will be the same in the final region where turbulent mixing predominates right to the wall. Differences in concentration at a given station will be only produced by the predominant conditions in the initial region as was shown in the preceding section.

Finally, the wall concentration distribution for a Newtonian fluid computed from [35] for $Re_x = 10^7$, is

$$\frac{c}{c_i} = 25.6\ \frac{v_i}{V}\ \frac{s}{x} \qquad [37]$$

an expression that is in remarkably good agreement with [5] and with other experimental formulae (20). The differences in

the power affecting the distance are not considerable and seem to be due to the simplification of the present model.

V. RELATIONSHIP BETWEEN CONCENTRATION DISTRIBUTION AND DRAG REDUCTION

The drag reduction attached to a drag reducing fluid injection will be related to the additive concentration close to the wall. Our experiments had shown that the wall concentration may be accurately measured and that the empirical data can be fitted by a quite accurate correlation. By using this correlation the concentration at the trailing edge of the plate is given by

$$c_L = 10.79 \left(\frac{v_i}{V}\right)^{1.74} \left(\frac{s}{L}\right)^{1.16} c_i^{2.16} \qquad [38]$$

if

$$L > 7.2 \left(\frac{v_i}{V}\right)^{1.5} s\, c_i \text{ , and}$$

$$c_L \simeq c_i$$

if

$$L < 7.2 \left(\frac{v_i}{V}\right)^{1.5} s\, c_i \text{ .}$$

Figure 16 shows the drag reduction values plotted against the trailing edge concentration computed from [38]. Although the number of experimental points, is not sufficient to establish an accurate correlation it could be said that maximum drag

reduction seems to be produced by values of the injected concentration and ratio of injection to free stream velocity, such that, the trailing edge concentration will be only a few parts per million. This corresponds in the present case to an injected concentration of 500 ppm and a velocity ratio of about 0.3. Increases of the injected concentration will not necessarily be accompanied by an increase of the drag reduction.

Direct comparisons with other measurements of drag reduction due to wall injection are difficult because the differences on the initial conditions that prevails upstream of the injection slot and the different geometries of the ejectors in the experimental set-ups. Nevertheless, let us compute the values of the trailing edge concentrations in the case of maximum drag reduction obtained by Wu and Tulin (10) for an injection of 300 ppm at an injection velocity of about one tenth of the free stream velocity

DR (%)	c (ppm)	v_i/V	L/s	c_L (ppm)
58	300	0.0980	10^3	13.2

The computed trailing edge concentration is larger, by an order of magnitude, than those estimated in the present experiments for high drag reduction efficiency.

In the case of Love's experiments we have,

DR (%)	c (ppm)	v_i/V	L/s	c_L (ppm)
43	50	0.317	532	4.87
47	50	0.422	532	8.10

values that are intermediate to those of Wu and Tulin and the present results.

From this, we can conclude that the trailing edge concentration is related to the drag reduction efficiency and that, by fixing its value, it is possible to compute the rate of injection of a drag reducing agent solution for a large range of free-stream velocities and lengths of the flat plate.

CONCLUSIONS

We have investigated experimentally the behavior of a tangential jet of concentrated solution of a drag reducing agent. Qualitative and quantitative explanations are offered for the initial and final regions of diffusion. By using the empirical formula that fit all the data obtained for the final zone it is shown that the drag reduction efficiency is related to the trailing edge concentration obtained for a given set of initial conditions - ejection velocity, width of the slot, free stream velocity and length of the plate from the injection

slot. Although the upstream conditions are very different for other experimental works it appears that the above relationship is verified within an order of magnitude on the trailing edge concentrations.

New experiments, particularly the measurement of the concentration profile normal to the wall, should be performed to increase the theoretical knowledge of the problem and to permit refinement of the present analysis.

ACKNOWLEDGEMENT

The authors wish to thank various members of the HYDRONAUTICS staff for their invaluable assistance in different phases of this work and particularly Dr. David Wiggert who designed the flat plate system and saw to its construction, to Mr. Newton Lewis who carried out many of the actual measurements, and to Dr. Sidney Reed and Dr. Jin Wu for their continually helpful interest and for their review of the manuscript.

REFERENCES

1. Toms, B. A., "Some Observations on the Flow of Linear Polymer Solutions Through Straight Tubes at Large Reynolds Numbers," Proc. 1st Intern. Congr. Rheol., 2, 135.

2. Tulin, M. P., "Hydrodynamic Aspects of Macromolecular Solutions," 6th Symposium Naval Hydrodynamics, Washington, 1966.

3. Lumley, J. L., Drag Reduction by Additives, Annual Review of Fluid Mechanics, 1, pp. 367-384, 1969.

4. Paterson, G. K., Zakin, J. L and Rodriguez, J M., "Drag Reduction," Industrial and Engineering Chemistry, Vol. 61, 1, January 1969, pp. 22-30.

5. Hoyt, J. W., and Fabula, A. G., "The Effect of Additives on Fluid Friction," Fifth Symposium on Naval Hydrodynamics, Bergen, Norway, 1964.

6. Wells, C. S., and Spangler, J. C., "Injection of a Drag-Reducing Fluids Into Turbulent Pipe Flow of a Newtonian Fluid," The Physics of Fluids, Vol. 10, No 9, pp. 1890-94.

7. Poreh, M., Rubin, H. and Elata, C., "Drag Reduction in a Developing Boundary Layer by Injection of Polymer Solutions," Technion, Israel, Hydraulics Dept Report No. 126, 1969.

8. Love, R. H., "The Effect of Ejected Polymer Solutions on the Resistance and Wake of Flat Plate in Water Flow," HYDRONAUTICS, Inc., Technical Report 353-2, June 1965.

9. Wu, J., "Drag Reduction in External Flow of Additive Solutions," in Viscous Drag Reduction, Plenum Press, 1969.

10. Wu, J. and Tulin, M. P., "Drag Reduction By Ejecting Additive Solutions into a Pure-Water Boundary Layer," HYDRONAUTICS, Inc., Technical Report 353-7, June 1970.

11. Tagori, T. and Ashidate, J., "Some Experiments on Friction Reduction of Flat Plate by Polymer Solution," 12th International Towing Tank Conference, Rome, 1969.

12. Johnson, V. E., Jr. and Goodman, A., "The HYDRONAUTICS Variable Pressure, Free Surface High-Speed Channel," Cavitation Research Facilities and Techniques, ASME, 1964.

13. Gollan, A., Tulin, M. P., and Rudy, S. L., "Development and Model Tests of a Surface Ship Additive System," HYDRONAUTICS, Inc., Tech. Rep. 909-1 FINAL, November 1970.

14. Seban, P. A., "Heat Transfer and Effectiveness for a Turbulent Boundary Layer with Tangential Fluid Injection," Journal of Heat Transfer, November 1960, pp. 303-312.

15. Levich, V. G., "Physicochemical Hydrodynamics," Prentice-Hall, Inc., 1962.

16. Schlichting, H., "Boundary Layer Thoery," McGraw-Hill Book Co., 1968.

17. Wells, S. C., "Turbulent Heat Transfer in Drag Reducing Fluids," AIChE Journal, 14, 522-525, 1966.

18. Elata, C., Lehrer, J. and Kahanovitz, A., "Turbulent Shear Flow of Polymer Solutions," Israel J. Technology, 4, No. 1, 87-95, 1966.

19. Fruman, D. and Sulmont, P., "Recherches sur la Reduction de la Resistance de Frottement en Hydrodynamique," Proc. ATMA, Paris, 1970.

20. Poreh, M. and Hsu, K. S., "Diffusion of Drag Reducing Polymers in a Turbulent Boundary Layer," J. HYDRONAUTICS, Vol. 6, No. 1, pp. 27-33, January 1972.

21. Giles, W. B., "Similarity Laws of Friction-Reduced Flows," Journal of HYDRONAUTICS, Vol. 2, No. 1, January 1968, pp. 34-40.

APPENDIX

POWER LAW VELOCITY PROFILE FOR DRAG REDUCING FLUIDS

Let us consider the turbulent flow in a pipe. The wall shear stress, τ_w, can be written as a function of a power law of the pipe Reynolds number, $V\,R/\nu$,

$$\frac{\tau_w}{\rho V_o^2} = c \left(\frac{\nu}{V\,R}\right)^{1/N} \qquad [A1]$$

and the shear velocity will be

$$u^{*\frac{2N-1}{N}} = c \left(\frac{\nu}{u^* R}\right)^{1/N} V^{\frac{2N-1}{N}} \qquad [A2]$$

By writing that the maximum velocity at the center of the pipe, U, is

$$U = k\,V \,. \qquad [A3]$$

we obtain

$$\frac{U}{u^*} = \frac{1}{c^{N/2N-1}\,k} \left(\frac{u^* R}{\nu}\right)^{\frac{1}{2N-1}} = \kappa \left(\frac{u^* R}{\nu}\right)^{1/n} \qquad [A4]$$

or

$$\frac{u}{u^*} = \kappa \left(\frac{u^* y}{\nu}\right)^{1/n} \qquad [A5]$$

Well known result that relate the power law of the velocity profile to the power law of the friction coefficient. From [45], the velocity profile is given by,

$$\frac{u}{U} = \left(\frac{y}{\delta}\right)^{1/n} \qquad [A6]$$

if R is replaced by δ, boundary layer thickness.

By following Schlichting (16) we have in the case of a flat plate,

$$\frac{\delta_1}{\delta} = \int_0^1 \left(1 - \frac{u}{U}\right) dy' = \frac{1}{n+1} \qquad [A7]$$

and

$$\frac{\delta_2}{\delta} = \int_1^{\delta} \frac{u}{U}\left(1 - \frac{u}{U}\right) dy' = \frac{n}{(n+1)\ (n+2)} \qquad [A8]$$

The wall shear stress on the flat plate surface will be

$$\frac{\tau_w}{\rho V^2} = c\left(\frac{\nu}{V\ \delta}\right)^{1/N} = \frac{n}{(n+1)\ (n+2)}\ \frac{d\delta}{dx} \qquad [A9]$$

that, by integration, allows the value of $\delta(x)$,

$$\frac{\delta(x)}{x} = \left[\frac{(n+1)\ (n+2)}{n}\left(\frac{N+1}{n}\right) c\right]^{\frac{N}{N+1}} \left(\frac{\nu}{Vx}\right)^{\frac{1}{N+1}} \qquad [A10]$$

The local friction coefficient, C_f, is given by

$$C_f = 2\left[\frac{(n+1)\ (n+2)}{n}\left(\frac{N+1}{N}\right) c\right]^{-\frac{1}{N+1}} \left(\frac{\nu}{Vx}\right)^{\frac{1}{N+1}} \qquad [A11]$$

1. Newtonian Fluid

The wall shear stress for a Newtonian fluid in a pipe is given by

$$\frac{\tau_w}{\rho V^2} = 0.0225 \left(\frac{\nu}{V\ R}\right)^{1/4}$$

and the velocity profile deduced from this expression is

$$\frac{u}{U} = \left(\frac{y}{\delta}\right)^{1/7}$$

By calculating the values of [A10] and [A11] with

$$c = 0.0025$$
$$N = 4$$
$$n = 7$$

we obtain the classical formulae

$$\frac{\delta(x)}{x} = 0.37 \left(\frac{\nu}{Vx}\right)^{1/5} \qquad [A12]$$

and

$$C_f = 0.0576 \left(\frac{\nu}{Vx}\right)^{1/5} \qquad [A13]$$

2. Drag Reducing Fluid

From the empirical data at minimum friction resistance, the law of friction is suggested (21) to be,

$$\frac{\tau_{w_p}}{\frac{1}{2}\rho V^2} = 0.545 \left(\frac{\nu}{V\ D}\right)^{0.5675} \qquad [A14]$$

This expression was verified by one of the authors (18) in the case of flow of Polyox WSR 301 in small pipes. From [A14] we obtain

$$\frac{\tau_{w_p}}{\rho V^2} = 0.4 \left(\frac{\nu}{V\ R}\right)^{0.5676} = 0.4 \left(\frac{\nu}{V\ R}\right)^{1/1.75} \qquad [A15]$$

The value of n will be,

$$n = 2N-1 = 2.5 \qquad [A16]$$

and by operating in [A10] and [A11], we have

$$\frac{\delta_p(x)}{x} = 2.4 \left(\frac{\nu}{Vx}\right)^{1/2.75} \qquad [A17]$$

and

$$C_{f_p} = 0.48 \left(\frac{\nu}{Vx}\right)^{1/2.75} \qquad [A18]$$

3. Relationship Between Wall Shear Velocities

The wall shear velocity u*, is related to the local friction coefficient by,

$$\frac{u^*}{U} = \sqrt{\frac{C_f}{2}} \qquad [A19]$$

From [A13] and [A18] we obtain the following ratio between the wall shear velocity produced by a homogeneous drag reducing solution and by the solvent

$$\frac{u^*_p}{u^*} = \frac{(0.24)^{\frac{1}{2}}}{(0.0288)^{\frac{1}{2}}} \left(\frac{\nu}{V R}\right)^{0.082} \qquad [A20]$$

For $Re_x \sim O(10^7)$ this ratio will be

$$\frac{u^*_p}{u^*} = 0.785 \qquad [A21]$$

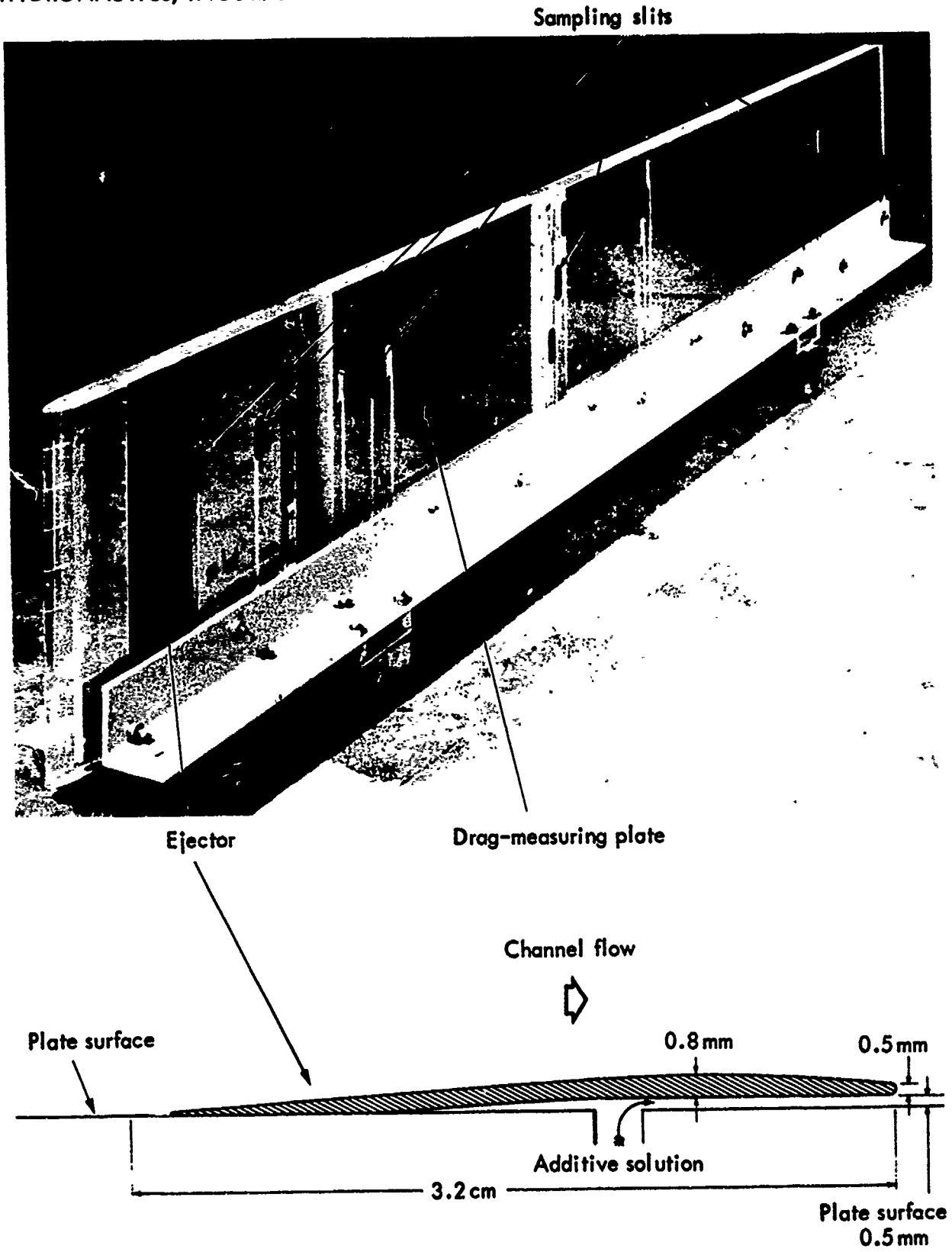

FIGURE 1 - LONG PLATE AND EJECTOR

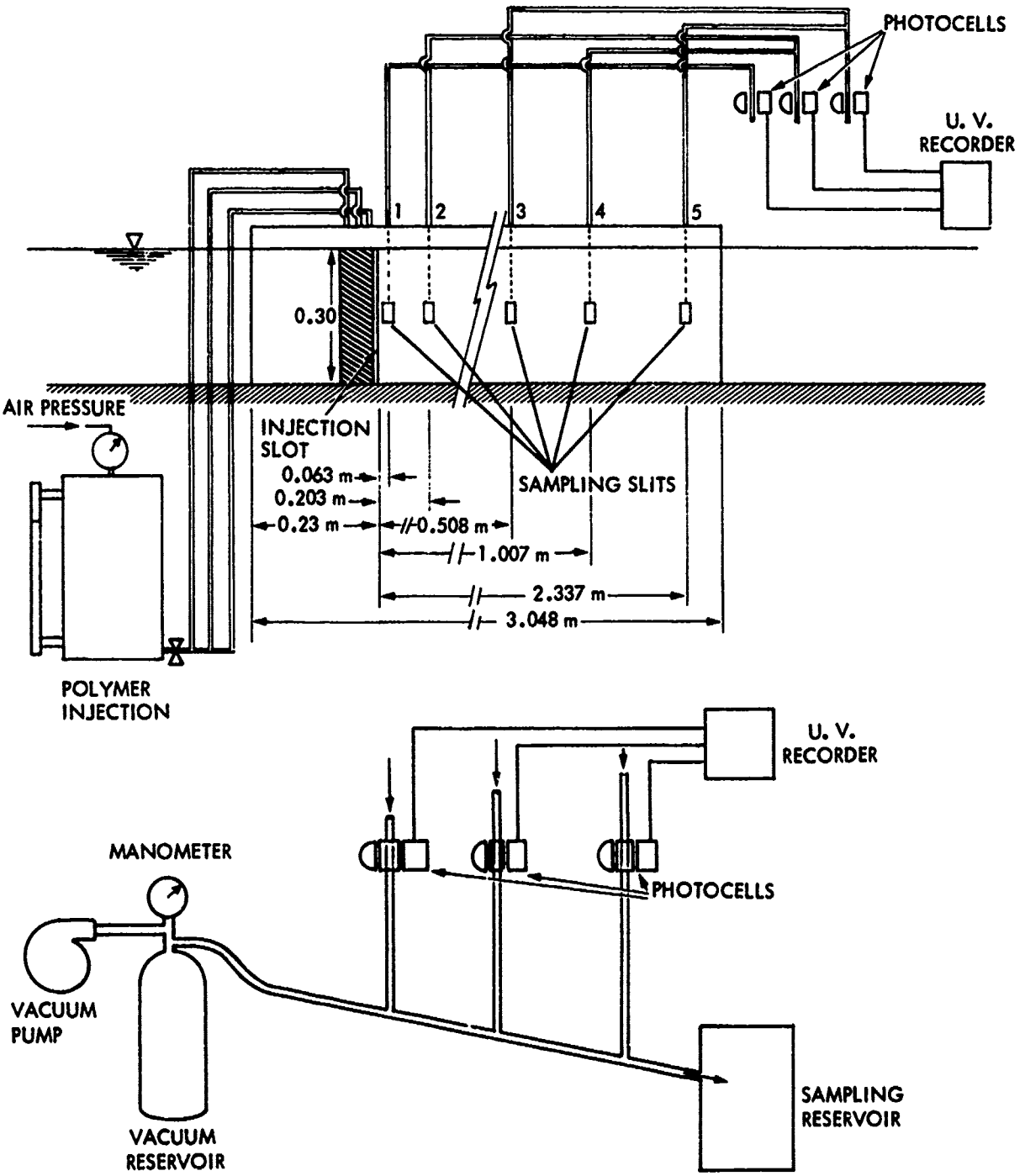

FIGURE 2 -EXPERIMENTAL SET-UP

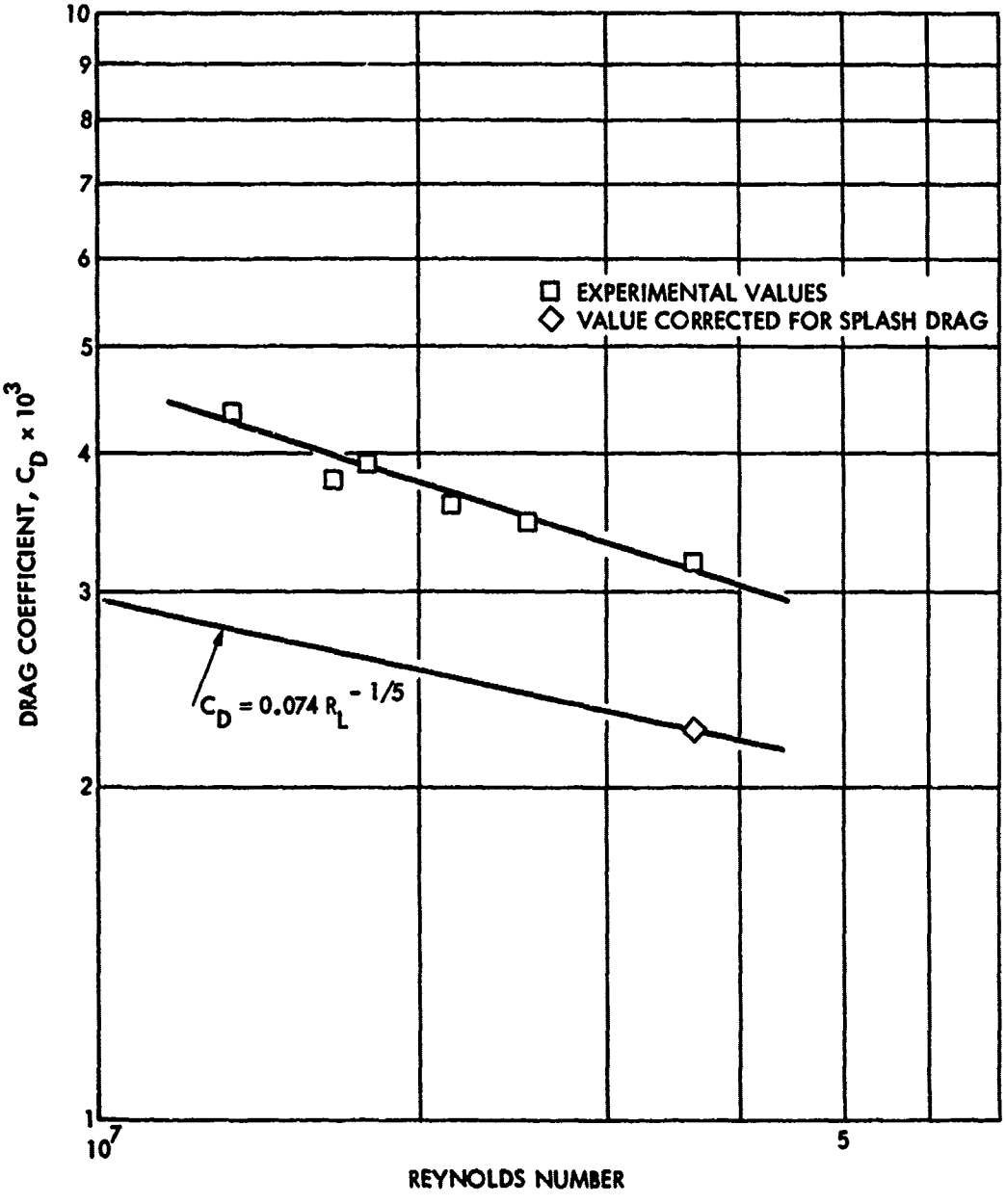

FIGURE 3 - FLAT PLATE DRAG VERSUS REYNOLDS NUMBER WITHOUT INJECTION

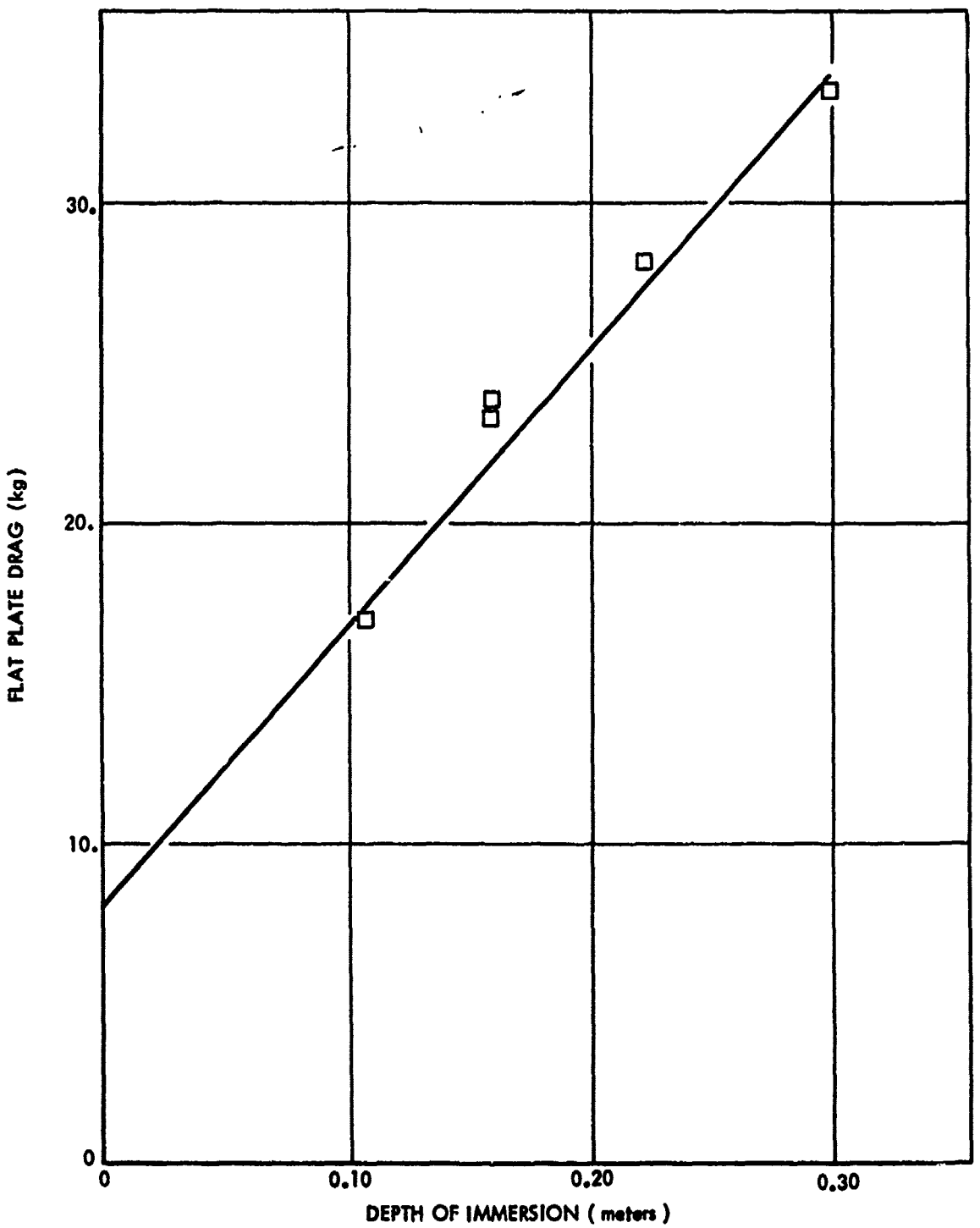

FIGURE 4 - FLAT PLATE DRAG VERSUS DEPTH

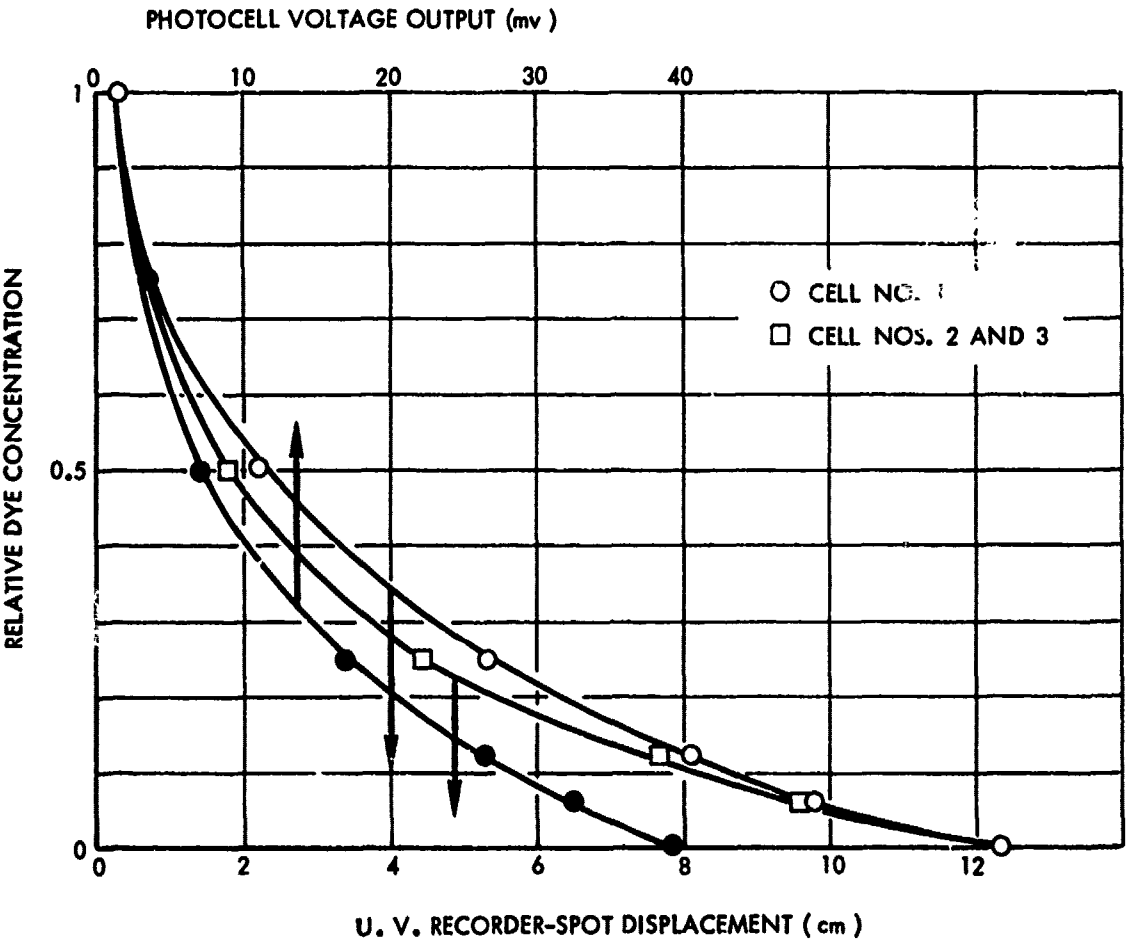

FIGURE 5 - CALIBRATION CURVES FOR LIGHT TRANSMISSION PHOTOCELLS

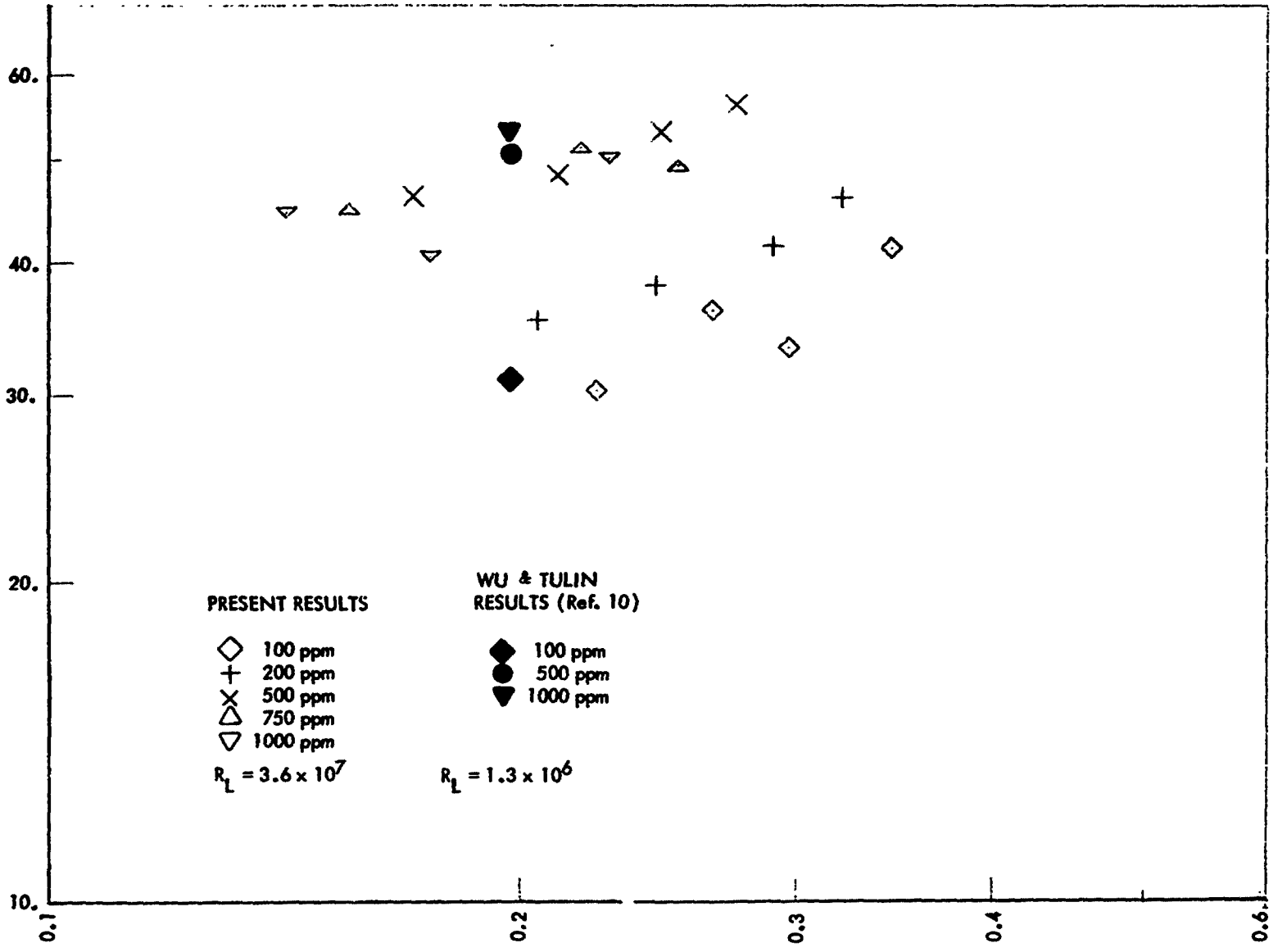

FIGURE 6 -DRAG REDUCTION BY A TANGENTIAL EJECTION OF POLYMER SOLUTIONS INTO A PURE WATER BOUNDARY LAYER OVER A SMOOTH SURFACE

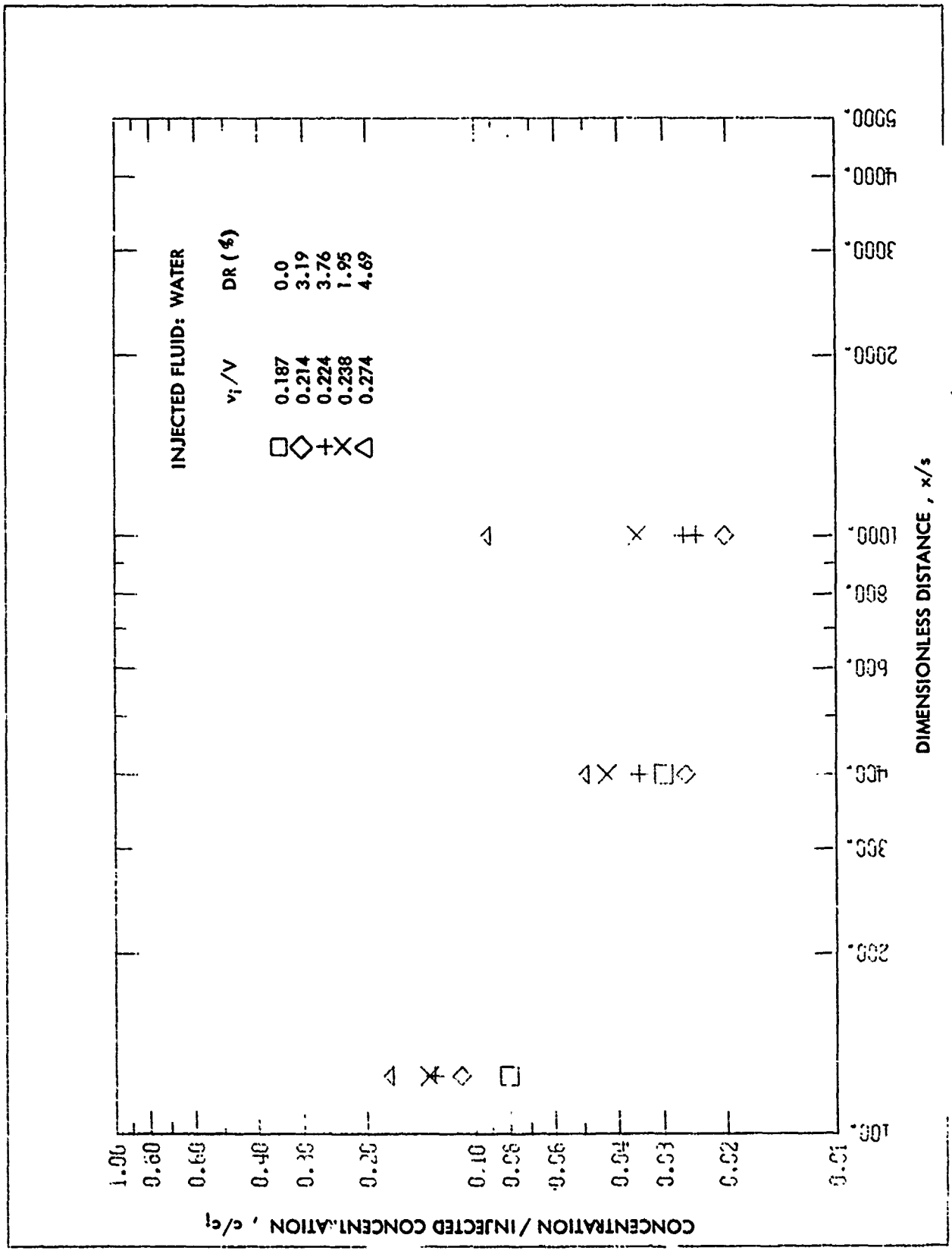

FIGURE 7 - CONCENTRATION OVER INJECTED CONCENTRATION RATIO, c/c_j , VS. DIMENSIONLESS DISTANCE, x/s, FOR WATER INJECTION.

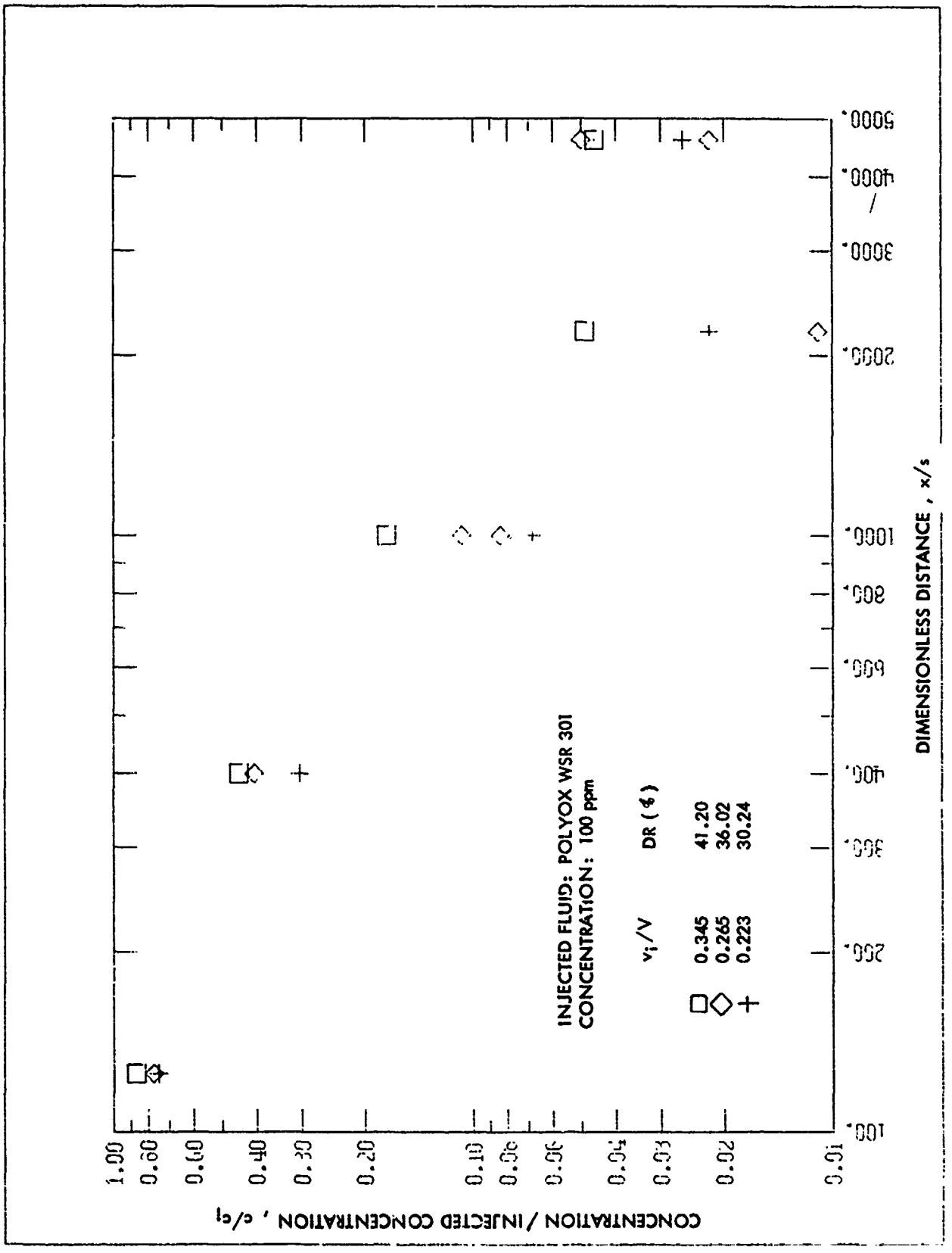

FIGURE 8 - CONCENTRATION OVER INJECTED CONCENTRATION RATIO, c/c_i , VS. DIMENSIONLESS DISTANCE, x/s, FOR 100 ppm POLYOX WSR 301 INJECTION.

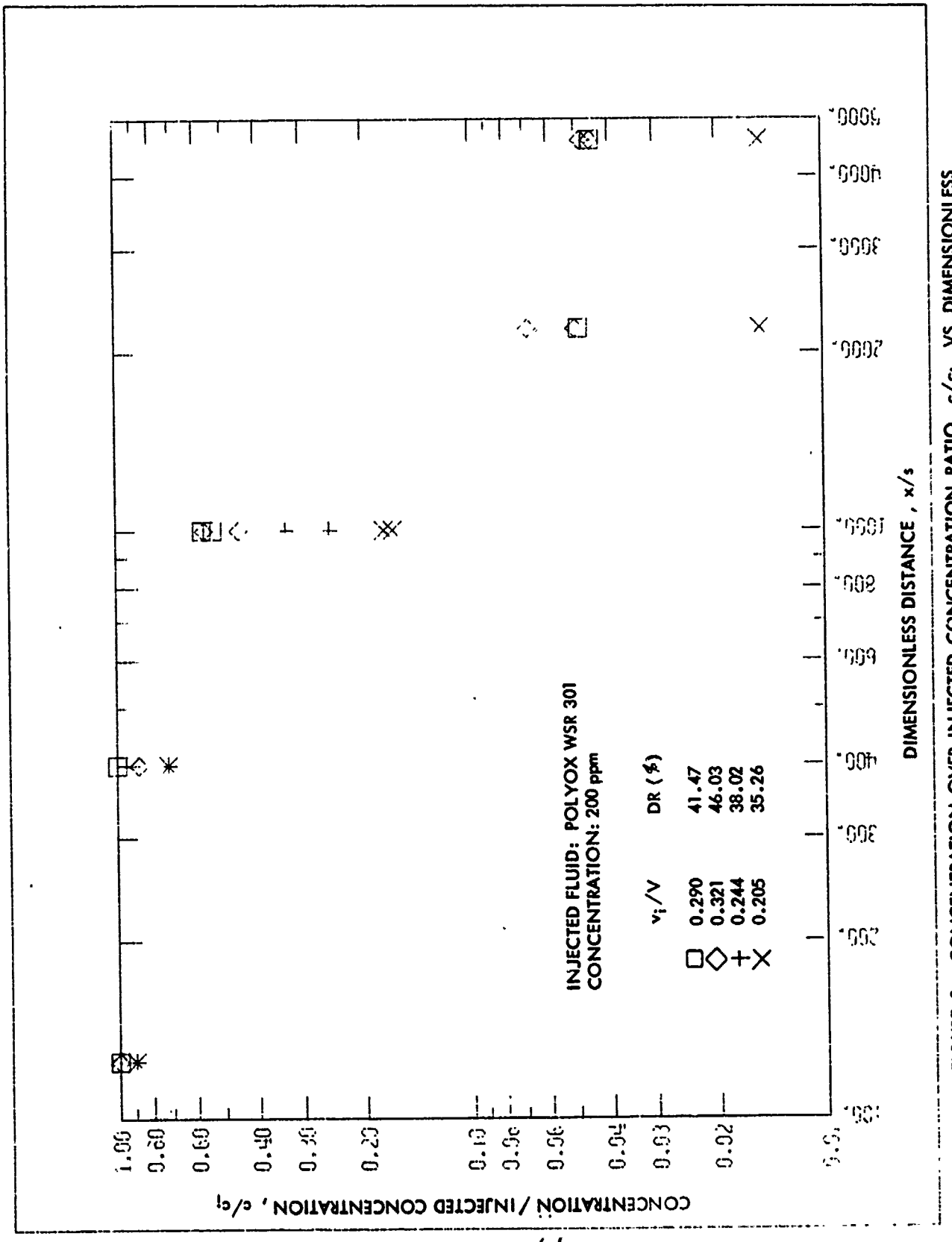

FIGURE 9 - CONCENTRATION OVER INJECTED CONCENTRATION RATIO, c/c_i, VS. DIMENSIONLESS DISTANCE, x/s, FOR 200 ppm POLYOX WSR 301 INJECTION.

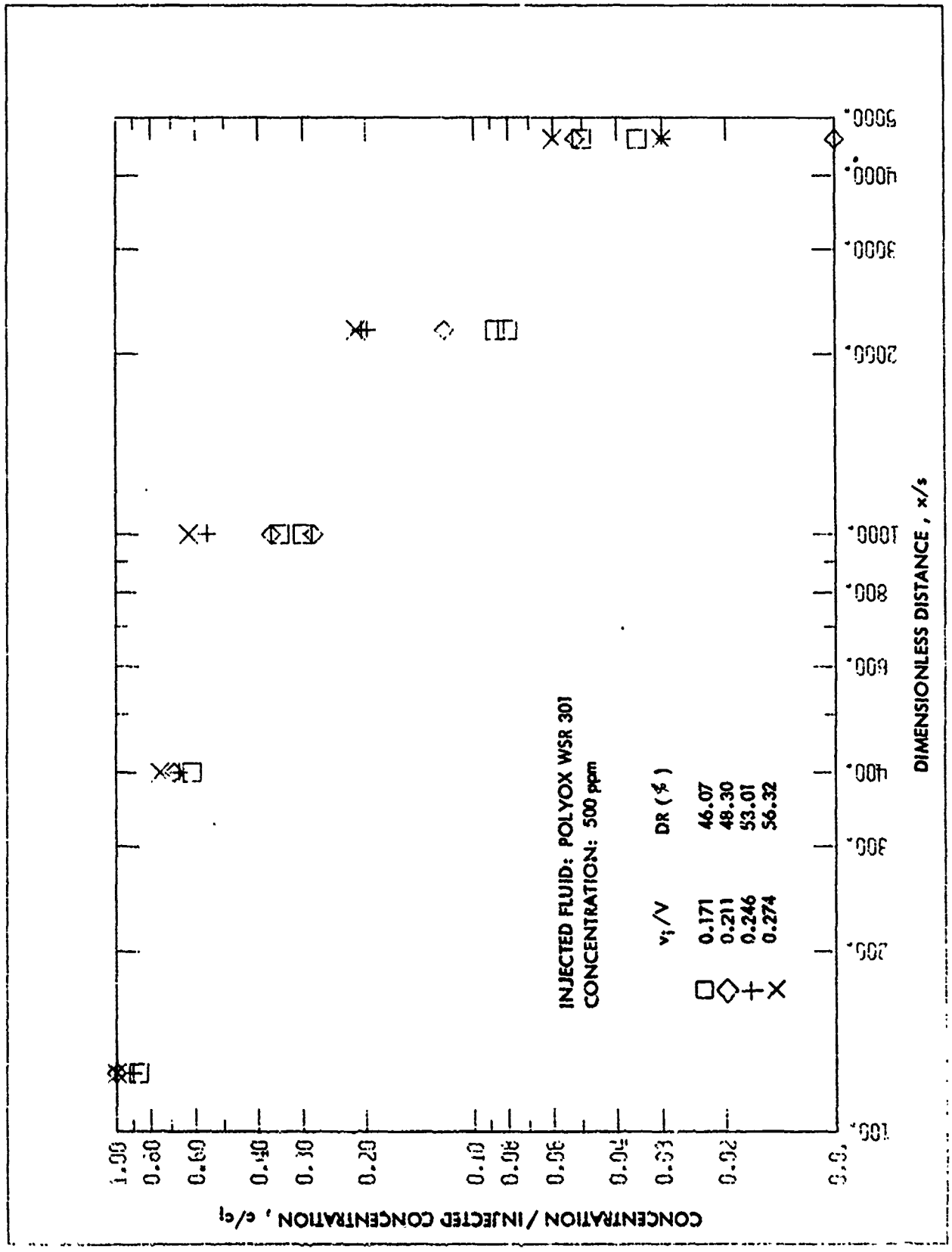

FIGURE 10 – CONCENTRATION OVER INJECTED CONCENTRATION RATIO, c/c_i, VS. DIMENSIONLESS DISTANCE, x/s, FOR 500 ppm POLYOX WSR 301 INJECTION.

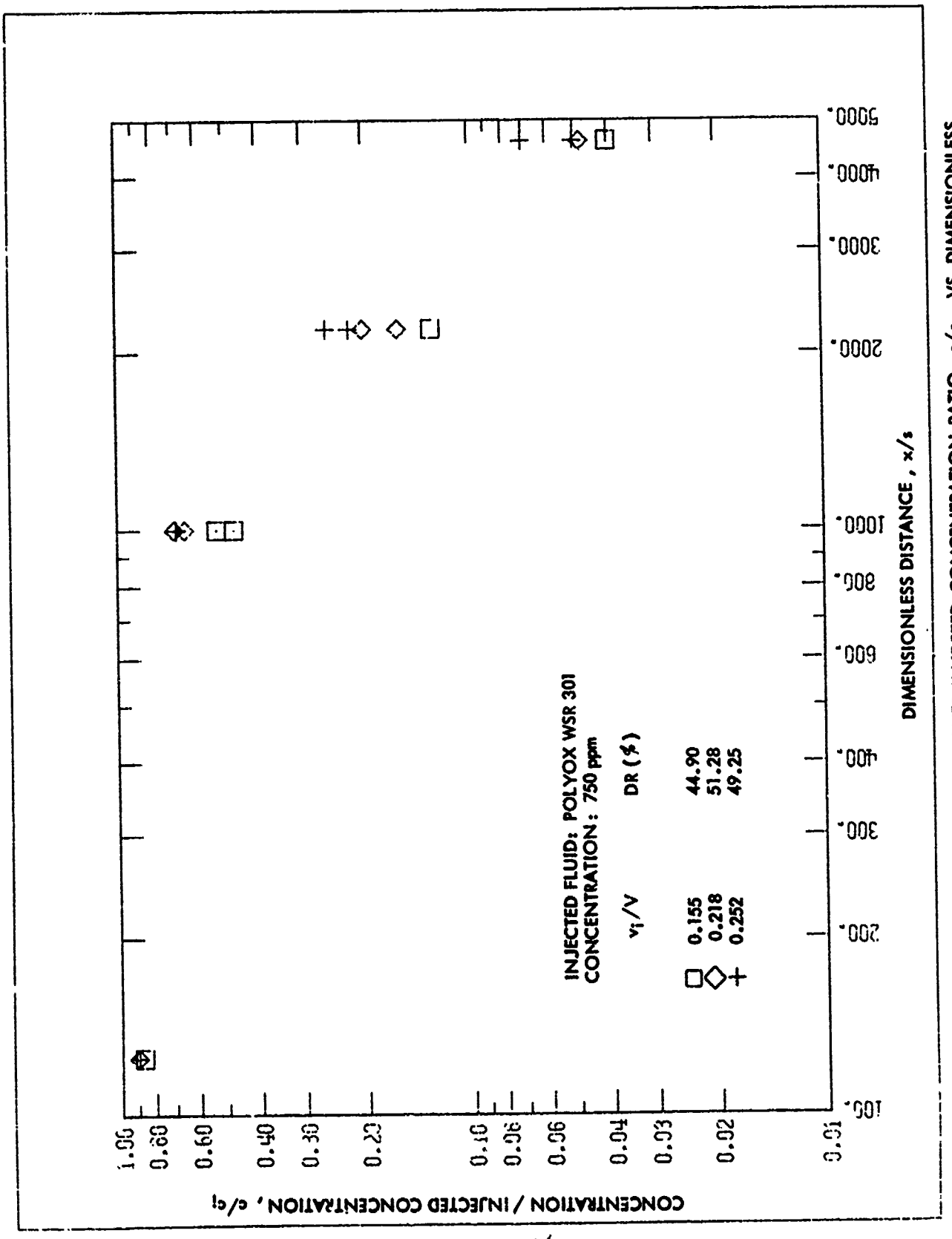

FIGURE 11 - CONCENTRATION OVER INJECTED CONCENTRATION RATIO, c/c_i, VS. DIMENSIONLESS DISTANCE, x/s, FOR 750 ppm POLYOX WSR 301 INJECTION.

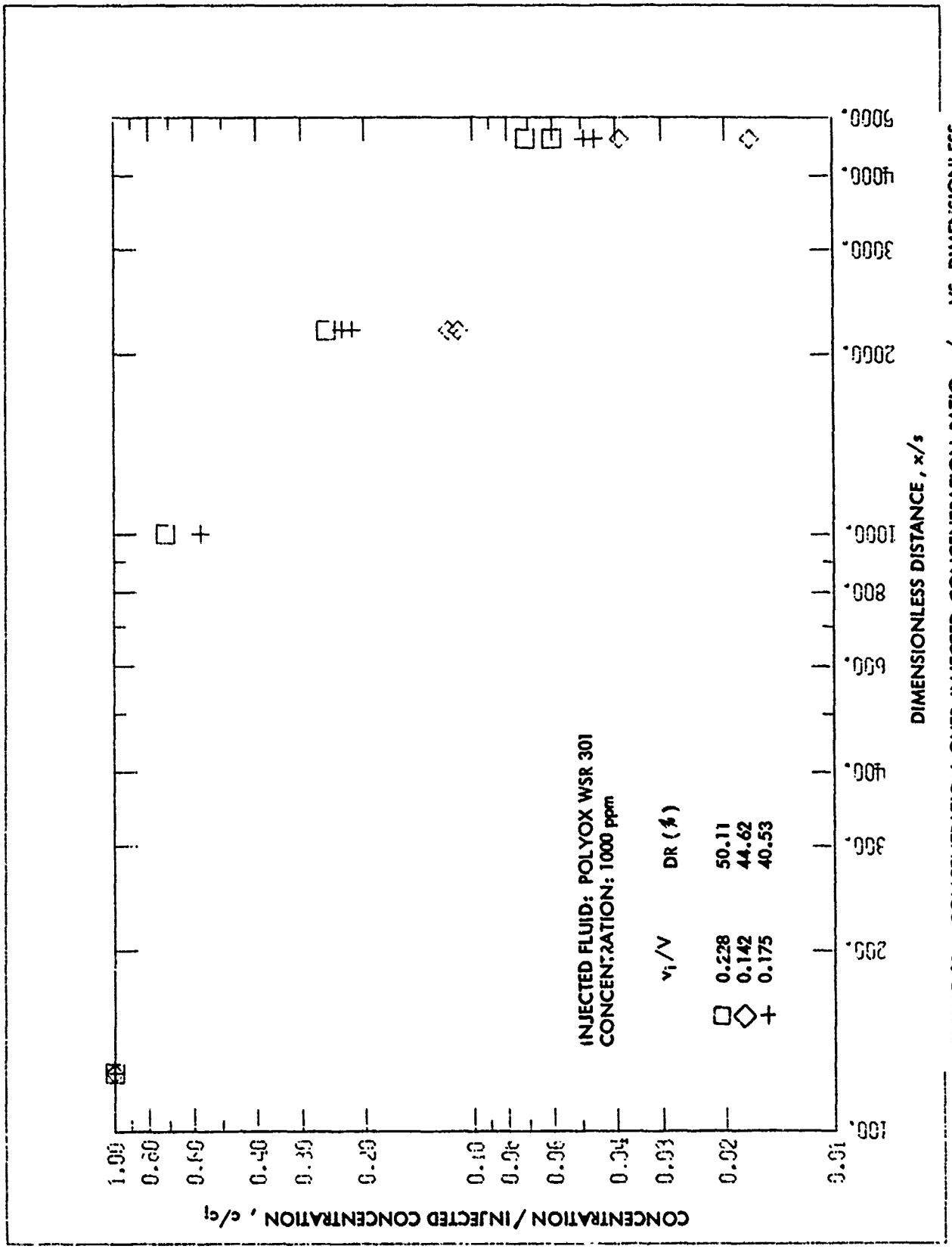

FIGURE 12 – CONCENTRATION OVER INJECTED CONCENTRATION RATIO, c/c_i, VS. DIMENSIONLESS DISTANCE, x/s, FOR 1000 ppm POLYOX WSR 301 INJECTION.

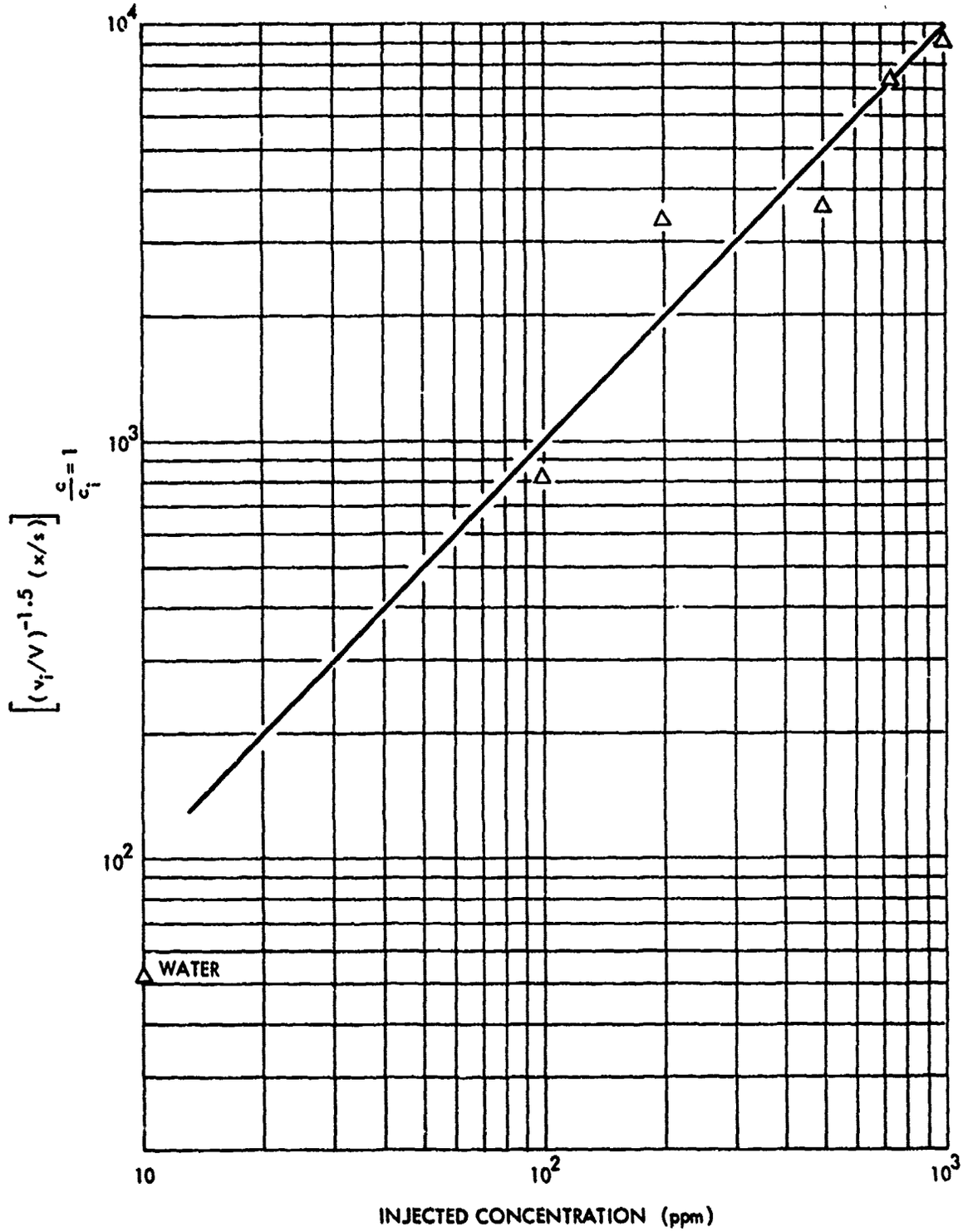

FIGURE 13 - INITIAL DISTANCE FOR FINAL ZONE VERSUS INJECTED POLYMER CONCENTRATION

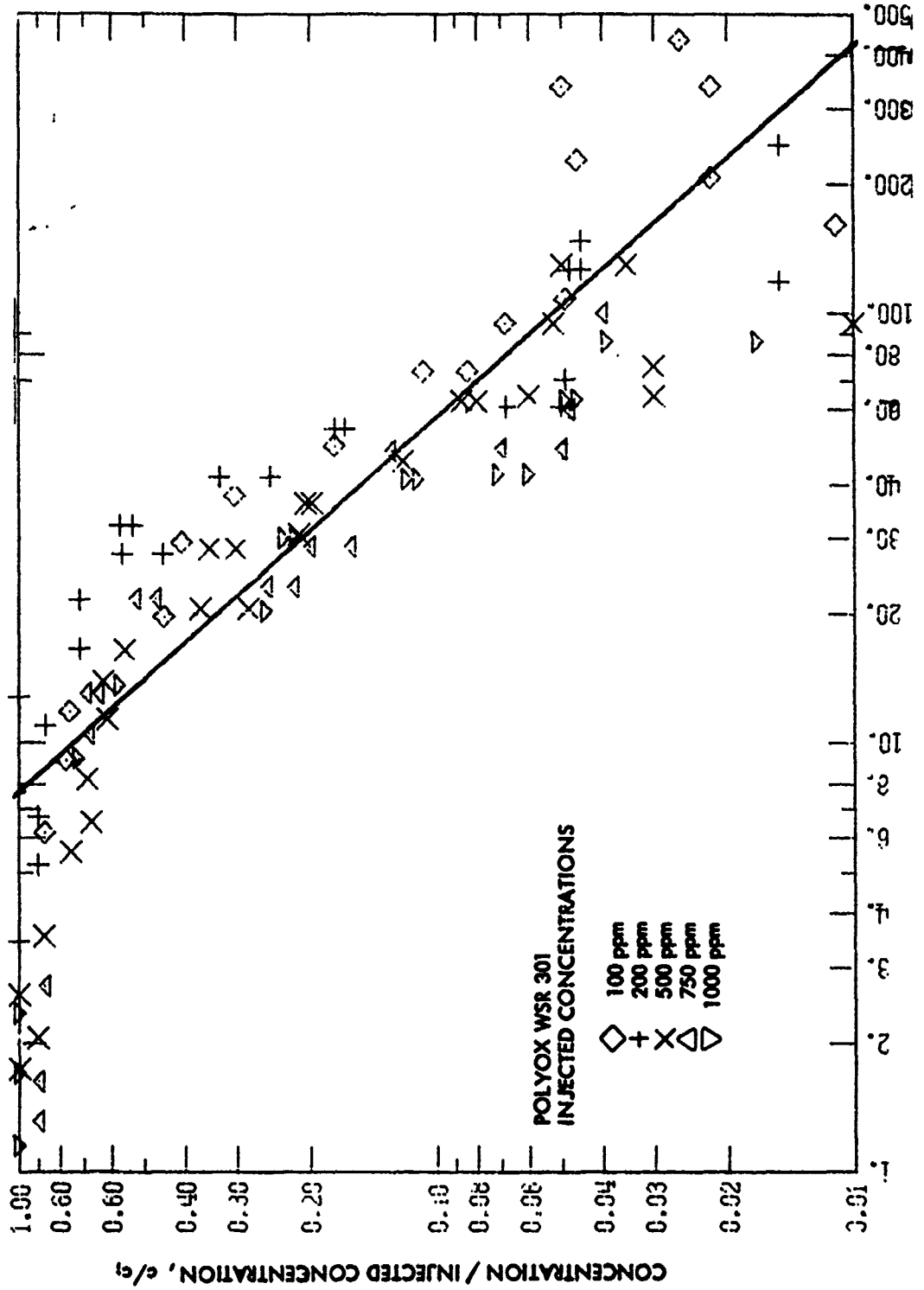

FIGURE 14 – DIMENSIONLESS CONCENTRATION VERSUS REDUCED DIMENSIONLESS DISTANCE

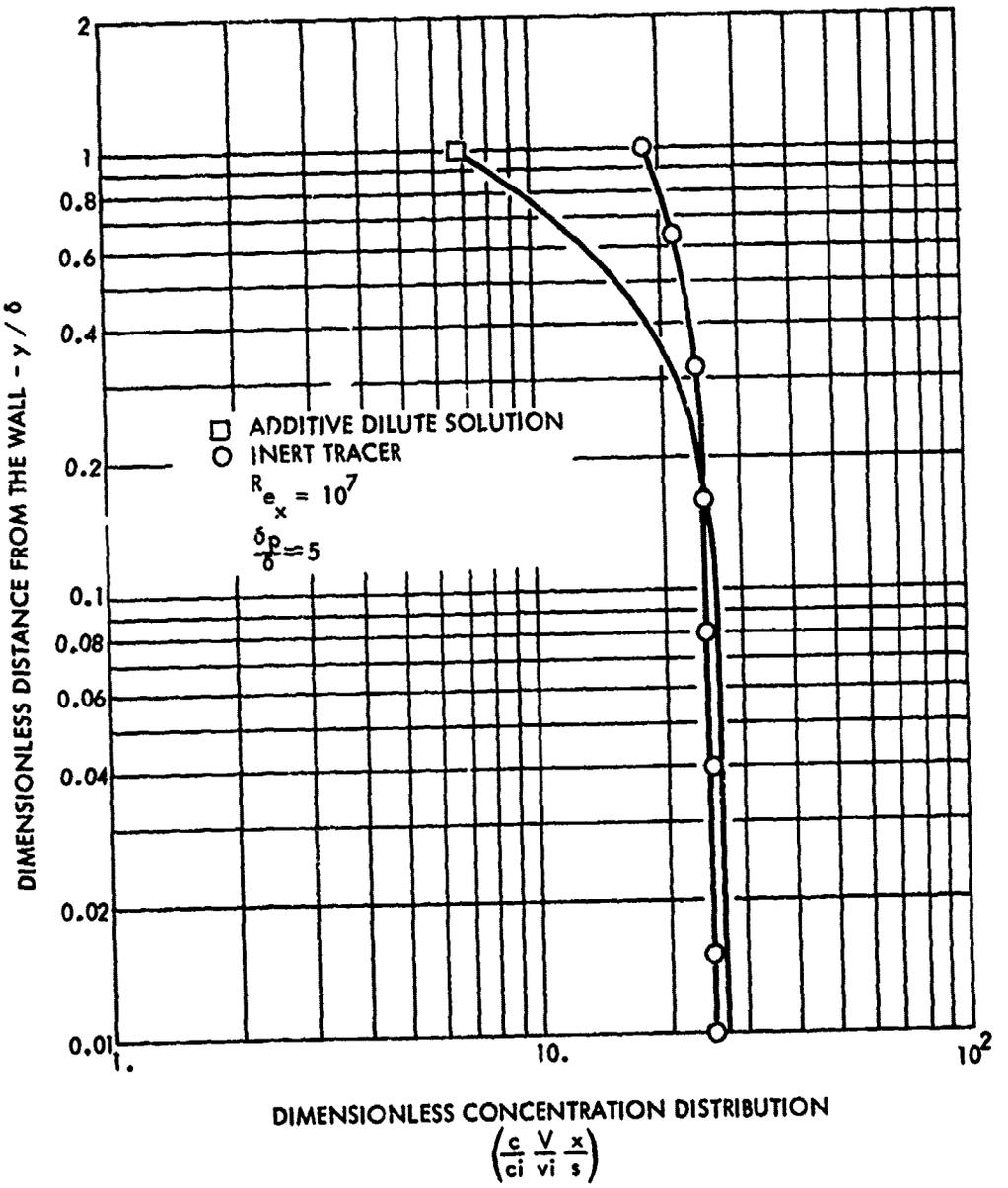

FIGURE 15 - CONCENTRATION PROFILE IN THE FINAL ZONE FOR INERT TRACER AND ADDITIVE INJECTION

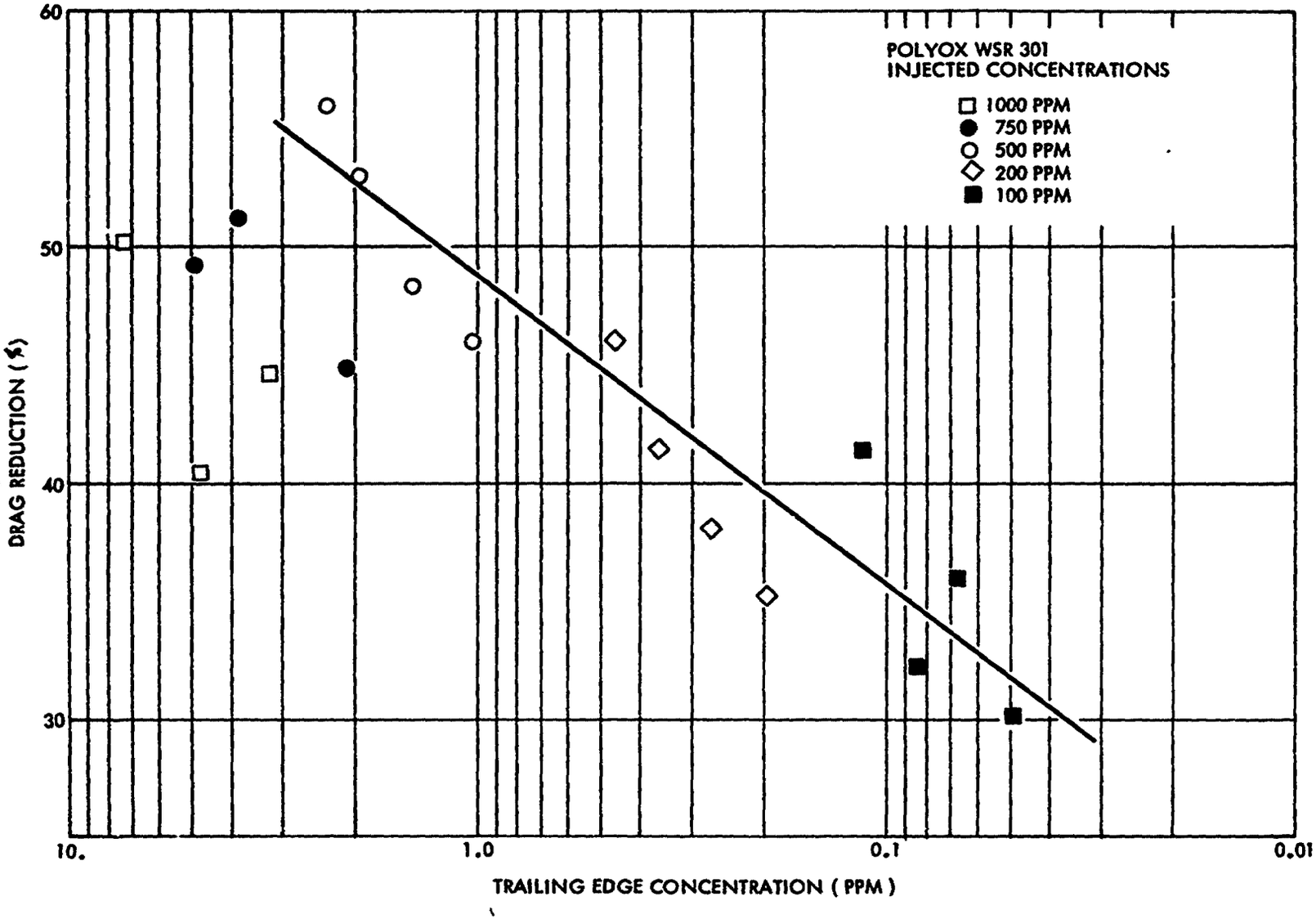

FIGURE 16 – DRAG REDUCTION VERSUS TRAILING EDGE CONCENTRATION